HAL
open science

Plant NADPH-dependent thioredoxin reductases are crucial for the metabolism of sink leaves and plant acclimation to elevated CO 2

Paulo Souza, Liang-yu Hou, Hu Sun, Louis Poeker, Martin Lehman, Humaira Bahadar, Adilson Domingues-Junior, Avilien Dard, Laetitia Bariat, Jean-philippe Reichheld, et al.

To cite this version:

Paulo Souza, Liang-yu Hou, Hu Sun, Louis Poeker, Martin Lehman, et al.. Plant NADPH-dependent thioredoxin reductases are crucial for the metabolism of sink leaves and plant acclimation to elevated CO 2. Plant, Cell and Environment, In press, 10.1111/pce.14631 . hal-04119116

HAL Id: hal-04119116

https://hal.science/hal-04119116v1

Submitted on 6 Jun 2023

HAL is a multi-disciplinary open access archive for the deposit and dissemination of scientific research documents, whether they are published or not. The documents may come from teaching and research institutions in France or abroad, or from public or private research centers.

L'archive ouverte pluridisciplinaire **HAL**, est destinée au dépôt et à la diffusion de documents scientifiques de niveau recherche, publiés ou non, émanant des établissements d'enseignement et de recherche français ou étrangers, des laboratoires publics ou privés.

Plant NADPH-dependent thioredoxin reductases are crucial for the metabolism of sink leaves and plant acclimation to elevated CO_2

Paulo V.L. Souza[1*], Liang-Yu Hou[2*], Hu Sun[3], Louis Poeker[2], Martin Lehman[2], Humaira Bahadar[1], Adilson P. Domingues-Junior[4], Avilien Dard[5], Laetitia Bariat[5], Jean-Philippe Reichheld[5], Joaquim Albenisio G. Silveira[1], Alisdair R. Fernie[4], Stefan Timm[3**], Peter Geigenberger[2**], Danilo M. Daloso[1**]

[1] LabPlant, Departamento de Bioquímica e Biologia Molecular, Universidade Federal do Ceará, Fortaleza 60451-970, Brazil

[2] Ludwig-Maximilians-University Munich, Faculty of Biology, 82152 Planegg-Martinsried, Germany.

[3] University of Rostock, Plant Physiology Department, Albert-Einstein-Straße 3, D-18059 Rostock, Germany

[4] Max Planck Institute of Molecular Plant Physiology, Am Mühlenberg 1, D-14476 Golm, Germany

[5] Laboratoire Génome et Développement des Plantes, Unité Mixte de Recherche 5096, Centre National de la Recherche Scientifique, Université de Perpignan Via Domitia, Perpignan, France

*** These authors contributed equally**

****Correspondence to:** daloso@ufc.br, geigenberger@bio.lmu.de and stefan.timm@uni-rostock.de

Running head: Characterization of plants lacking all NTR isoforms

Summary Statement: We unveil that NTRC is crucial for sink leaf metabolism and plant acclimation to high CO_2. Although Arabidopsis plants lacking all NTRs have severely reduced growth, they produced viable seeds, indicating that NTRs are not essential for plant development and compensated by other redox mechanisms.

Abstract

Plants contain three NADPH-thioredoxin reductases (NTR) located in the cytosol/mitochondria (NTRA/B) and the plastid (NTRC) with important metabolic functions. However, mutants deficient in all NTRs remained to be investigated. Here, we generated and characterized the triple Arabidopsis *ntrabc* mutant alongside with *ntrc* single and *ntrab* double mutants under different environmental conditions. Both *ntrc* and *ntrabc* mutants showed reduced growth and substantial metabolic alterations, especially in sink leaves and under high CO_2 (HC), as compared to the wild type. However, *ntrabc* showed higher effective quantum yield of PSII under both constant and fluctuating light conditions, altered redox states of NADH/NAD^+ and glutathione (GSH/GSSG) and lower potential quantum yield of PSII in sink leaves in ambient but not high CO_2 concentrations, as compared to *ntrc*, suggesting a functional interaction between chloroplastic and extra-chloroplastic NTRs in photosynthesis regulation depending on leaf development and environmental conditions. Our results unveil a previously unknown role of the NTR system in regulating sink leaf metabolism and plant acclimation to HC, while it is not affecting full plant development, indicating that the lack of the NTR system can be compensated, at least to some extent, by other redox mechanisms.

Key words: Fluctuating light, metabolic regulation, plant acclimation to high CO_2, redox metabolism, redox regulation, sink leaves.

Introduction

Plants have an unprecedented redox system that allow these organisms to rapidly respond to changes in environmental cues (Geigenberger *et al.* 2017). Light absorption rapidly alters the redox state of the chloroplasts by increasing the level of redox active molecules such as NAD(P)H, reduced ferredoxin (Fdx) and H_2O_2 (Elsässer *et al.* 2020; Ugalde *et al.* 2021). It is noteworthy, however, that H_2O_2 production is not strictly dependent on light availability, given that several biochemical reactions in the peroxisomes, the mitochondria electron transport chain and the activity of NADPH and other oxidases can produce H_2O_2 in the dark (Lampl *et al.* 2022). H_2O_2 is an oxidant, acting as an important regulator of plant metabolism by modulating gene expression and altering enzyme activity through the oxidation of cysteine (Cys) residues in redox-sensitive proteins (Foyer *et al.* 2020). This process is counter-balanced by thioredoxins (TRXs), ubiquitous proteins involved in redox regulation of plant metabolism by modulating Cys thiol–disulphide exchange in target proteins (Meyer *et al.* 2021). Plant redox metabolism is thus orchestrated by redox reactions, which aid plants to rapidly respond to changes in environmental signals, including those associated to the climate change scenario (Mhamdi & Noctor 2016).

Plant TRXs depend on reducing power derived from TRX reductases, which use either photosynthetically Fdx or NADPH as electron donors, according to the subcellular location (Meyer *et al.* 2009). In the chloroplasts, Fdx and NADPH are respectively used by Fdx-dependent TRX reductases (FTRs) and the NADPH-dependent TRX reductase C (NTRC), which also harbour a TRX domain in its structure (Evans *et al.* 1966; Serrato *et al.* 2004). Although NTRC and FTRs comprise distinct pathways, they act cooperatively regulating chloroplastic metabolism by activating different TRX isoforms present in this organelle (Thormählen *et al.* 2015; Yoshida & Hisabori 2016a). Plants further possess two other NTRs, namely NTRA and NTRB, which are the major TRX reductases outside of the plastids (Laloi *et al.* 2001; Reichheld *et al.* 2005, 2007). The plant NTR/TRX system is thus an important hub for metabolic regulation by directly (de)activating a suit of redox-regulated enzymes in different subcellular compartments, some of which are related to important physiological process such as photosynthesis and photorespiration (Martí *et al.* 2020; Cejudo *et al.* 2021). For instance, whilst several Calvin-Benson-Bassham (CBB) cycle enzymes are activated by the chloroplastic FDX/TRX system, enzymes related to the mitochondrial (photo)respiratory metabolism such as glycine

decarboxylase (GDC), fumarase and succinate dehydrogenase are deactivated by the NTR/TRX system (Fonseca-Pereira *et al.* 2021). It is expected therefore that NTR proteins may have an important role for plant high CO_2 (HC) acclimation. However, the mechanisms by which the redox metabolism aid plants to acclimate HC condition remains unclear (Foyer & Noctor 2020).

Compared to animal cells, plants have a higher number of different TRX and TRX reductase isoforms, residing in different subcellular compartments (Foyer & Noctor 2020). Whilst only one TRX reductase is found in mammalian mitochondria, plants possess two NTR proteins (NTRA and NTRB) in this organelle, as result of a genetic duplication (Blanc *et al.* 2000; Reichheld *et al.* 2005). This leads to a higher robustness of the plant redox network compared to animal cells. For instance, whilst the knockout of the mitochondrial TRX reductase is lethal for mammalian cells (Conrad *et al.* 2004), Arabidopsis plants lacking either NTRC or both NTRA and NTRB are smaller than wild type (WT) plants, but still viable (Serrato *et al.* 2004; Reichheld *et al.* 2007; Daloso *et al.* 2015). The restricted growth of *ntrab* and *ntrc* mutants have been associated to alterations in the carbon metabolism within the cytosol and mitochondria (Daloso *et al.* 2015) and mainly to a reduced photosynthetic capacity, respectively, especially under fluctuating light conditions (Thormählen *et al.* 2017). NTR proteins are thus highly important for plant growth. However, NTRC and the non-chloroplastic NTRA/B systems are safeguarded by FTRs and glutathione reductases (GR), respectively, which may act as compensatory systems and guarantee the viability of *ntrc* and *ntrab* mutants (Marty *et al.* 2009, 2019). Indeed, it has been shown that glutathione (GSH) can reduce plant TRXs *in vitro* and that NTRA/NTRB and GR act in cooperation (Reichheld *et al.* 2005, 2007, Marty *et al.* 2009, 2019). This indicates that the plant NTR/TRX system is highly connected to other redox players, including glutathione and ascorbate metabolisms (Calderón *et al.* 2018). However, it remains unclear whether the deficiency of NTRA and NTRB has additional consequences for the *ntrc* mutant, and *vice versa*, and whether the complete lack of the entire NTR system is severely affecting plant growth, development and viability.

As the whole plant metabolism and, especially, redox reactions operate in a highly integrated and dynamic manner in response to endogenous and environmental cues, it is crucial to understand the interactions that occur between the three plant NTR isoforms. Considering this, we have obtained a triple NTR mutant (*ntrabc*) by crossing the *ntrc*

single mutant with the double *ntrab* mutant in Arabidopsis. We characterized these plants alongside with WT, *ntrc* single and *ntrab* double mutants by analysing the regulation of growth, photosynthesis and both primary and redox metabolisms under different environmental conditions. In light of our previous findings, showing that TRX *o1* and *h2* contribute to the regulation of photorespiratory metabolism (Reinholdt *et al.* 2019b; Fonseca-Pereira *et al.* 2020), we included experiments under two different CO_2 concentrations. These experiments were carried out in order to distinguish direct and indirect effects resulting only from a compromised NTRC system (high CO_2, 3000 ppm, supressed photorespiration) from those possibly resulting from impaired regulation of photorespiration (normal air, 400 ppm CO_2, active photorespiration). Our results indicate a previously unknown role of the plant NTR system, especially the chloroplastic NTRC protein, in the regulation of sink leaf metabolism and plant acclimation to high CO_2. Being crucial to maintain growth rates under different CO_2 concentrations or fluctuating light conditions, our data highlight NTR isoforms being not essential for full plant development.

Material and methods

Plant material and growth conditions

Seeds from *Arabidopsis thaliana* (Arabidopsis) L. Columbia (Col-0) and T-DNA insertional mutants *ntrc* (SALK_012208) and *ntrab* (NTRA SALK_539152, NTRB SALK_545978) were obtained from SALK collection (http://signal.salk.edu/) and characterized previously (Serrato *et al.* 2004; Reichheld *et al.* 2007; Daloso *et al.* 2015; Thormählen *et al.* 2015). The *ntrabc* triple mutant was obtained by crossing the single *ntrc* with *ntrab*. Seeds were germinated as described previously (Fonseca-Pereira *et al.* 2020) and sown in soil containing sand, vermiculite, and organic substrate Topstrato® (1:1:1). Plants were grown under approximately 120 µmol photons m^{-2} s^{-1} of constant light and different photoperiods (8/16,12/12 or 16/8 h light/dark), as indicated in each legend of the figures. Beyond these conditions, plants were also grown under fluctuating light (FL), which comprised a loop of alternating low light (LL; 50 µmol photons m^{-2} s^{-1} for 5 min) and high light (HL; 550 µmol photons m^{-2} s^{-1} for 1 min) phases, as well as under 400 ppm (ambient air – referred here as normal CO_2 concentration - NC) or 3000 ppm (high CO_2, HC) of CO_2. The CO_2 concentration was selected based on previous

studies, revealing almost all photorespiratory mutants restore to wild type performance at 3000 ppm CO_2 (summarized in Timm & Bauwe 2013). Entire rosettes from these experiments were collected and frozen in liquid nitrogen for further analysis, as highlighted in the legend of each figure.

Growth analysis

Plants were harvested to determine plant size (cm^2), fresh (FW) and dry (DW) weights (mg) and the DW-to-FW ratio. The size of entire rosettes was measured using the software Photoshop (Adobe Photoshop®). Prior to the measurement of dry weight, the entire rosette was dried out in an oven (60°C) for 48 h. We further determined the number of leaves and the rosette diameter of plants grown under normal (NC) or high (HC) CO_2 conditions. The relative changes in number of leaves and rosette diameter were calculated in HC-grown plants as compared to the NC-grown plants (HC-to-NC ratio).

Protein extraction and immunoblots

Arabidopsis protein extracts were prepared by grinding approximately 150 mg of fresh weight leaf material in liquid nitrogen and resuspended in extraction buffer (25 mM Tris HCl, pH 7.6, 75 mM NaCl, 1 mM DTT, 1 mM phenylmethylsulfonyl fluoride, and 0.1% Nonidet P-40). After centrifugation (15 min, 18,700 *g*, 4°C), protein concentrations from the supernatant were determined using the Protein Assay kit (Bio-Rad). Proteins were separated by SDS-PAGE and transferred to Immobilon-P membranes (Amersham Pharmacia). Rabbit polyclonal antibodies against NTRB (Reichheld *et al.* 2007) and NTRC (Serrato *et al.* 2004) were diluted 1:10,000 for protein gel blotting. Goat anti-rabbit antibodies conjugated to horseradish peroxidase (Amersham Pharmacia) were used as secondary antibodies and revealed with enhanced chemiluminescence reagents (Amersham Pharmacia).

Pulse-amplitude-modulation (PAM) measurements of chlorophyll *a* fluorescence

Plants were dark-acclimated for 30 min and then transferred into an image PAM (MAXI version, Heinz-Walz Instruments, Effeltrich, Germany) instrument. Plants were treated with 150 μmol photons $m^{-2}s^{-1}$ for 20 min followed by darkness for 10 min. For the measurement under FL, plants were treated with 4 min low light followed by 4 cycles of FL comprising 1 min high light phases (500 μmol photons $m^{-2}s^{-1}$) and 6 min low light phases (50 μmol photons $m^{-2}s^{-1}$), and then the dark for another 5 min. The emission of

florescence was documented by the image PAM and used to estimate the effective quantum yield of photosystem II [Y(II)], non-photochemical quenching (NPQ) and the reduction of plastoquinone pool (1-qL), as described earlier (Thormählen *et al.* 2017). The minimal fluorescence (F_0) and the potential quantum yield of the photosystem II (F_v/F_m) of dark-adapted leaves was determined in all genotypes using plants grown under NC and HC conditions using an imaging PAM (M-series, Heinz-Walz Instruments, Effeltrich, Germany).

Gas exchange analysis

Gas exchange analysis was carried out on fully expanded leaves from 8-week-old plants using portable infra-red gas exchange analysers (Li-Cor 6400XT; Li-Cor, Lincoln, NE, USA). The net CO_2 assimilation rate (A), the CO_2 compensation point (Γ), stomatal conductance (g_s), substomatal CO_2 concentration (C_i), transpiration rate (E), and the ratio between substomatal and ambient CO_2 concentration (C_i/C_a) were obtained from light and CO_2 response curves. The maximum electron transport rate (J) was estimated as described previously (Sharkey 2016). The responses of A and J to different light intensities were best fitted into the following regression equation: $Y = a\,(1 - e^{-bx})$, where Y represents A or J parameters.

GC-TOF-MS-based metabolite profiling analysis

Polar metabolites were extracted from leaves harvested at end of the day (ED) and end of the night (EN) and derivatized following a well-established gas chromatography-*time of flight* - mass spectrometry (GC-TOF-MS) platform (Lisec *et al.* 2006). Metabolites were identified using the TagFinder 4.1 software and the Golm Metabolome Database (Kopka *et al.* 2005; Luedemann *et al.* 2008). The data presented corresponds to the intensity of specific fragments of the metabolites normalized by the fresh weight (g) used for metabolite extraction and the intensity of the internal standard (ribitol/^{13}C-Sorbitol) added during the extraction (Lisec *et al.* 2006).

LC-MS/MS-based metabolite profiling analysis

Liquid chromatography coupled to tandem mass spectrometry (LC-MS/MS)-based metabolite profiling was carried out in source and sink leaves from selected genotypes (WT, *ntrc*, *ntrab* and *ntrabc*) grown in NC or HC conditions. Leaves from plants at the growth stage 5.1 (Boyes *et al.* 2001) were harvested at ED, frozen in liquid nitrogen and stored at -80°C until further analysis. The identification and the

determination of metabolite concentration was carried out through LC-MS/MS exactly as described previously (Reinholdt *et al.* 2019b).

Measurement of starch and soluble sugars

The content of starch and soluble sugars was measured as described previously (Hendriks *et al.* 2003). Briefly, polar metabolites were extracted from 20 mg of ground leaf material using 80% (v/v) ethanol. After 30 min at 90ºC, a centrifugation was made (10 min at 20,000 *g* at 25ºC). The supernatant and the remaining pellet were then used for the quantification of soluble sugars and starch, respectively. The concentration of starch, glucose, fructose and sucrose was determined through the formation of NADPH from the glucose-6-phosphate dehydrogenase (G6PDH) reaction by a spectrophotometer at 340 nm (FilterMax F5, Molecular Device).

Determination of reduced and oxidized glutathione and ascorbate contents

The contents of oxidized (DHA), reduced (ASC) and total ascorbate (DHA + ASC) was determined as described previously (Kampfenkel *et al.* 1995). In brief, leaves harvested at ED and EN were ground to a powder using liquid nitrogen. The method is based on the reduction of Fe^{+3} into Fe^{+2} by ASC and spectrophotometric detection of the Fe^{+2} complex bound to 2,2'-pirydine, being monitored by decrease of the ASC absorbance at 525 nm. Both ASC and DHA forms were expressed as μmol mg^{-1} fresh weight (FW) calculated from ASC standard curve. GSH was measured by the GSH reductase (GR)-dependent reduction of 5,5′-dithiol-bis (2-nitrobenzoic acid), DTNB (Griffith 1980). The content of GSH and GSSG was expressed as μmol g^{-1} FW and calculated using a standard curve of GSH.

Pyridine nucleotides determination

The pyridine nucleotides assays were based on the selective hydrolysis of the reduced forms (NADH and NADPH) in an acid medium and of the oxidized forms (NAD^+ and $NADP^+$) in an alkaline medium (Lintala *et al.* 2014). Pyridine nucleotides were determined using the phenazine methosulfate-catalysed reduction of dichlorophenolindophenol in the presence of ethanol and alcohol dehydrogenase (for NAD^+ and NADH) or glucose 6-phosphate (G6P) and G6P dehydrogenase (G6PDH) (for $NADP^+$ and NADPH), as described earlier (Lintala *et al.* 2014).

Determination of superoxide dismutase, catalase and ascorbate peroxidase activities

Total proteins were extracted by adding 1 ml of potassium phosphate buffer (100 mM; pH 7.0) containing EDTA (final concentration of 1 mM) in tubes containing powder of frozen leaves. The homogenate was centrifuged at 15,000 *g* at 4°C for 15 min, and the resulting supernatant was used for the determination of all enzymatic activities. The total content of soluble proteins was measured according to Bradford (Bradford 1976). All enzymatic activities were determined spectrophotometrically. Superoxide dismutase activity (SOD) was determined based on the inhibition of tetrazolium chloride (NBT) nitro blue chloride photoreduction (Giannopolitis & Ries 1977). The unit of SOD activity (U) was defined as the amount of enzyme needed to inhibit 50% of NBT photoreduction, expressed as U mg^{-1} FW min^{-1}. Catalase activity (CAT) was measured by reduction of H_2O_2 (Beers & Sizer 1952; Havir & McHale 1987). CAT activity was calculated using the molar extinction coefficient of H_2O_2 (40 mM cm^{-1}) and expressed as mmol H_2O_2 mg^{-1} FW min^{-1}. The activity of ascorbate peroxidase (APX) was measured based on the oxidation of ASC, in a reaction mixture containing 0.45 mM of ASC, 3 mM of H_2O_2, and 50 µl of the protein extract, all diluted in a buffer of potassium phosphate 100 mM (pH 7.0) containing 1 mM EDTA in a final volume of 1.5 ml (Nakano & Asada 1981). APX activity was expressed in µmol ASC mg^{-1} FW min^{-1}.

Detection of hydrogen peroxide

The H_2O_2 content was quantified using the Red Hydrogen Peroxide / Peroxidase Amplex Assay kit (Life Technologies, Carlsbad, CA, United States) according to the manufacture's protocols. In brief, 100 µl of protein extract was mixed with 100 µl of the Amplex red solution (Amplex-red 0.2 M +HRP 0.2 U + potassium phosphate buffer 100 mM; pH 7.5). The absorbance was measured at 560 nm to quantify the H_2O_2 concentration (Zhou *et al.* 1997). The results were expressed as nmol H_2O_2 mg^{-1} FW.

Statistical analysis

All measurements were performed with at least four biological replicates. All graphs were generated using GraphPad Prism 9. Heat maps were created using the MeV 4.9.0 software. The genotypes were compared by analysis of variance (ANOVA) followed by Tukey or Dunnet tests or by Student's *t* test ($P < 0.05$). Metabolomics data was analysed by hierarchical clustering analysis (HCA) and principal component analysis (PCA) using MeV 4.9.0 software and the Metaboanalyst platform, respectively. Pearson correlation analysis was also carried out using the Metaboanalyst platform (Pang *et al.* 2021).

Results

Plant growth, but not development, is severely impaired in plants lacking the complete set of NTR proteins

We obtained an Arabidopsis mutant lacking all three NTR isoforms (*ntrabc*) through crossing of the single *ntrc* and the double *ntrab* mutant. The deletion of NTR proteins in the *ntrabc* line was confirmed by immunoblotting using antibodies against NTRC and NTRA+B (Supplemental Figure S1a). The triple *ntrabc* mutant displayed a similar pale-green phenotype as *ntrc* line if grown under either, constant medium light (ML) (~120 µmol m^{-2} s^{-1}) or fluctuating light (FL) (50 µmol m^{-2} s^{-1} for 5 min; 550 µmol m^{-2} s^{-1} for 1 min) conditions, respectively (Figure 1a). Furthermore, *ntrabc* plants - similar to *ntrc* - showed reduced plant growth when compared to WT and *ntrab*, as indicated by lower fresh weight (FW), dry weight (DW) and plant size under ML and FL. Although the mean of plant size of *ntrc* was 2.3 and 1.3-fold higher than *ntrabc* under ML and FL conditions, respectively, no statistical difference was found in growth parameters between these mutants, with exception of the DW-to-FW ratio that was lower in *ntrabc* than *ntrc* (Figure 1b). Interestingly, although *ntrabc* plants showed reduced plant growth, they could complete their life cycle, from vegetative to reproductive stages (Figure S1b). These results collectively indicate that the lack of NTRA and NTRB do not exacerbate biomass production caused by the absence of NTRC and highlight that NTR proteins are not essential for full Arabidopsis development.

Impaired photochemical capacity in the single *ntrc* mutant is attenuated in the *ntrabc* triple mutant

Plants lacking *ntrc* have reduced photosynthetic capacity (Thormählen *et al.* 2015). We therefore investigated whether the additional lack of both NTRA and B causes additional photosynthetic impairment in *ntrabc* plants. Gas exchange analysis demonstrated that, compared to WT and *ntrab*, *ntrc* and *ntrabc* mutants had more drastic reductions in the rates of CO_2 assimilation (*A*) and maximum electron transport rate (*J*) (Figure S2a-b). The reduction in *A* was associated to a reduced stomatal conductance (g_s) and, by consequence, lower transpiration rate (*E*) in *ntrc* and *ntrabc* mutants, when

compared to WT and *ntrab* (Table S1). CO_2 response curves showed that both *ntrc* and *ntrabc* mutants had higher CO_2 compensation points than WT and *ntrab* (Table S1). During dark-light transitions, both *ntrc* and *ntrabc* were found to have reduced effective quantum yield of PSII (Y(II)) and elevated levels in the reduction of plastoquinone pool (1-qL) and in non-photochemical quenching (NPQ), when compared to WT and *ntrab* (Figures 1c-e). However, during the first 10 min of the transition, Y(II) was surprisingly higher and NPQ lower in *ntrabc* compared to *ntrc* plants (Figures 1c-d). The differences between *ntrabc* and *ntrc* mutants with respect to these photosynthetic parameters were enhanced when plants were analysed in alternating low light (LL) and high light (HL) phases in FL, compared to constant medium light. Under these conditions, the photosynthetic levels in the *ntrabc* triple mutant ranged between those of WT and *ntrc* single mutant (Figures S3a-c). These results indicate that during transient changes in light intensity, the photosynthetic phenotype of the *ntrabc* triple mutant is less severe, compared to the *ntrc* single mutant.

Leaf primary metabolism is substantially altered in *ntrc* and *ntrabc* triple mutants depending on the light conditions

We next investigated the consequences of NTRs absence on primary metabolism by analysing the metabolite profiles in leaf samples harvested at the end of the day (ED) and end of the night (EN) using GC-TOF-MS. The metabolite profile of *ntrabc* plants was largely comparable to *ntrc* at ED. Twenty-one and twenty out of forty-three metabolites identified were significantly different in *ntrc* and *ntrabc*, respectively, if compared to WT at ED. This statement is in line with both hierarchical clustering analysis (HCA) (Figure 2a) and principal component analysis (PCA), in which a clear separation of both *ntrc* and *ntrabc* plants from WT and *ntrab* was observed by the PC1 (Figure 2b). On the other hand, ten and seventeen metabolites were significantly different in *ntrab* and *ntrabc* at EN, respectively, if compared to WT (Figure 2a). However, HCA demonstrated that *ntrabc* is more similar to *ntrc* than *ntrab* and the PCA showed no clear separation among the genotypes at EN (Figures 2a,c). Among the metabolites altered in *ntrabc* leaves, considerable decreases were found in the abundances of carbohydrates, including glucose and fructose. Therefore, we further investigated how the lack of NTRs affect the concentration of starch and soluble sugars (glucose, fructose and sucrose) by using a

spectrophotometric method. Reduced concentrations of starch, glucose and sucrose was observed in both *ntrc* and *ntrabc* plants, if compared to WT at ED. However, no difference was seen between the *ntrabc* mutant and the other genotypes at EN (Figures S4a-h).

Given that the differences in photosynthesis and growth between the mutants and the WT are attenuated under FL conditions, we next investigated whether this is also observed at metabolic level. We carried out another GC-MS-based metabolite profiling analysis in leaves harvested at the middle of the day (MD) and EN of plants grown under constant medium light (ML) condition and at the low light (LL), high light (HL) and dark phases (EN) after the transition to FL (Figure S5). HCA and PCA strengthen the idea that the metabolic phenotypes of *ntrc* and *ntrabc* are substantially different from WT and *ntrab* when plants are grown under constant light (ML), as evidenced by the HCA clusters in the heat maps (Figure S5) and the genotypes separation by the PC1, especially at MD (Figure 3). However, these metabolic distinctions between genotypes were less severe in FL compared to ML, which is in-line with the growth analyses in these light conditions. While there were no substantial changes between the metabolite profiles of *ntrc* and *ntrabc* mutants in both light conditions, there is obviously no clear metabolic explanation for the different photosynthetic efficiencies of these mutants observed in FL. However, the metabolite data are overall levels and do not reflect changes in different subcellular compartments.

Growth impairment of *ntrc* and *ntrabc* mutants is further associated to disruptions in photosynthesis and metabolism of sink leaves in either ambient or high CO_2

Given that the photosynthetic phenotypes of *ntrabc* and *ntrc* were different to WT and *ntrab* plants under various light conditions, we further carried out a chlorophyll *a* fluorescence analysis of these mutants in other environmental conditions and in leaves of different developmental stages. This involved analyses via imaging PAM of dark-adapted sink and source leaves of *ntrc*, *ntrab*, and *ntrabc* mutants grown under either normal (ambient) (NC; 400 ppm) or high CO_2 (HC; 3000 ppm) concentrations alongside with the WT (Figures 4a-b). Interestingly, lower potential quantum yield of the photosystem II (F_v/F_m) and higher minimal fluorescence of dark-adapted leaves (F_0) were observed in sink leaves of both *ntrc* and *ntrabc* mutants grown under either NC or HC conditions,

when compared to WT and *ntrab* plants (Figures 4c-f). By contrast, no differences in F_v/F_m and F_0 were observed between the source leaves of the genotypes, with exception of the F_0 of *ntrabc* source leaves that was higher than WT source leaves under NC condition (Figure 4e). The F_v/F_m and F_0 of sink leaves were lower and higher in *ntrabc* than *ntrc* under NC, respectively, indicating a more severe photosynthetic restriction on sink leaves of the triple *ntrabc* mutant under these conditions (Figures 4c, e).

We also measured growth-related parameters including the rosette diameter and leaf-number of these plants. All mutant lines were smaller and had less leaves than WT under NC or HC conditions, with *ntrc* and *ntrabc* had much more severe growth phenotypes in HC. Interestingly, *ntrabc* plants were smaller and had less leaves than both *ntrab* or *ntrc* lines under NC, but not HC conditions (Figures 5c-d). Moreover, whilst WT and *ntrab* increased 10% and 18% in rosette diameter under HC, respectively, when compared to NC (**$P < 0.001$), *ntrc* was 29% smaller under HC than NC (**$P < 0.001$) (Figure 5e). Similarly, the number of leaves increased approximately 15% in WT and *ntrab* and decreased approximately 10% in *ntrc* under HC, when compared to NC (*$P < 0.05$) (Figure 5f). This demonstrates that the lack of NTRC or NTRAB have negative and positive effects for HC acclimation, respectively. Given this, neither the rosette diameter nor the number of leaves were altered by HC in *ntrabc*, when compared to NC (see Figures 5e-f). Considering the relative HC-to-NC changes between the genotypes, only the *ntrc* was different from the WT in both rosette diameter and number of leaves, whilst *ntrabc* showed reduced values of rosette diameter than the WT (see letters in the Figures 5e-f).

These analyses indicate that the exacerbated growth impairment of *ntrabc* plants under LC is also related to a reduced photochemical capacity of sink leaves, which may have severe consequences for the metabolism of these leaves. Therefore, we next carried out a liquid chromatography coupled to tandem mass spectrometry (LC-MS/MS)-based metabolite profiling analysis in source and sink leaves of *ntrc*, *ntrab* and *ntrabc* plants grown under NC or HC conditions. The results demonstrated that the impact of NTRC mutation is more severe in sink than source leaves, as indicated by the separation of *ntrc* and *ntrabc* from WT and *ntrab* by the PCA1 in both NC and HC conditions (Figure 6). This separation is mostly due the higher concentration of certain metabolites related to nitrogen metabolism including Arg, Asn and histidine (His), and lower concentrations of Ser, Gly, pyruvate, citrate/isocitrate, fumarate and succinate observed in sink leaves of

both *ntrc* and *ntrabc* plants, as compared to sink and source leaves of the WT and the source leaves of these mutants under either NC or HC conditions (Figure 7, Figure S6a-d). Interestingly, the Gly/Ser ratio was higher in sink than source leaves only in WT under NC. However, this ratio was much higher in sink leaves of both *ntrc* and *ntrabc* plants than WT source and sink leaves under HC condition (Figure S6e-f). Taken together, these results indicate that the lack of NTR proteins substantially alter nitrogen, organic acids and photorespiratory metabolism, especially in sink leaves, which contribute to the explanation of the reduced growth of *ntrc* and *ntrabc* specifically under HC condition.

The lack of NTRs alters the NADH/NAD$^+$ balance in illuminated leaves

The metabolism of pyridine dinucleotides is closely associated to the NTR system, since NAD(P)H is used as electron donors to reduce TRXs (Møller *et al.* 2020; Cejudo *et al.* 2021). Therefore, we investigated whether the lack of NTRs alters the overall level of pyridine nucleotide amounts (NAD$^+$, NADP$^+$, NADH, and NADPH) in leaf samples harvested at ED or EN. No differences in the concentrations of NADP$^+$, NADPH or total NADP(H) between the genotypes was observed in ED or EN (Figures S7a-f). Similarly, no clear differences were observed in the concentrations of NAD$^+$, NADH and total NAD(H) between the genotypes (Figures S7g-m), with the exception of NADH which was elevated in the *ntrabc* mutant compared to all other genotypes at ED (Figure S7h). When the concentration of these compounds was analysed in relative terms (%), no difference in NADP$^+$ and NADPH at ED and EN and in NAD$^+$ and NADH at EN was observed between the genotypes. However, *ntrabc* plants had a lower % of NAD$^+$ and higher % of NADH than WT at ED (Figures S8a-d), revealing that the lack of NTRs perturbs the proportion of leaf NAD$^+$ and NADH produced at ED.

The absence of NTRs strongly reduce the activity of antioxidant enzymes, leading to H_2O_2 over-accumulation at night

NTRC is an important hub for the redox metabolism (López-Grueso *et al.* 2019; Souza *et al.* 2019), we next investigated whether H_2O_2 content and the activity of antioxidant enzymes were altered in *ntr* mutants. Interestingly, our results showed that the major alterations were observed at EN, and, to a lesser extent, at ED. The H_2O_2 content and the activity of superoxide dismutase (SOD) was unaltered in *ntrabc* plants at ED,

when compared to WT plants (Figures 8a-b). However, all mutants showed lower activity of both ascorbate peroxidase (APX) and catalase (CAT), when compared to WT plants at ED (Figures 8c-d). In contrast, the content of H_2O_2 was higher, while the activity of SOD, APX and CAT was lower in all mutants at EN, if compared to WT (Figures 8e-h). These results collectively indicate that the knockout of NTRs directly affects ROS metabolism, in which reduced activity of ROS-scavenging enzymes leads to an over-accumulation of H_2O_2 at EN.

The relative levels of GSH and GSSG are altered in *ntrabc* plants at night

To further enhance our understanding about the role of NTRs for the regulation of redox metabolism, we quantified the concentrations of ascorbate (ASC), dehydroascorbate (DHA) and oxidized (GSSG) and reduced (GSH) glutathione in leaf samples harvested at ED and EN. No changes in the concentration of ASC or DHA between *ntrabc* and the WT were observed in either ED or EN, although significant changes in these molecules were present in *ntrc* and *ntrab* at EN. At ED, *ntrc* plants showed lower ASC and higher DHA than WT (Figures 9a-c, f-h), leading to a decrease in the ASC percentage of the total ASC pool (Figure S9). No major changes in GSH and GSSG between *ntrabc* and the WT was found, with the exception of GSSG which was 6.5-fold higher in *ntrabc* than WT at EN (Figures 9d-e, i-j). By analysing the percentage of oxidized DHA and GSSG related to their reduced forms (ASC and GSH), the unique differences between WT and *ntrabc* plants was the percentage of GSH and GSSG found at EN, in which *ntrabc* have higher GSSG and lower GSH compared to the control (Figure S9). By contrast, all parameters were different between *ntrc* and the WT, while *ntrab* showed much lower and higher % of ASC and DHA than the WT at EN (Figure S9).

Interestingly, whilst the level of H_2O_2 was not correlated with redox-related parameters at ED, H_2O_2 was negatively correlated with the activity of CAT and APX at ED and positively correlated with the concentration of GSSG at EN (Figure 10a-b). Furthermore, PCA using H_2O_2 and antioxidant-related parameters revealed a clear separation of the different genotypes at ED (specifically between *ntrc* and *ntrabc*), while that the major differences between WT and the mutants was present at EN (Figures 10c-

d). Collectively, these results highlight that NTR proteins are key for the regulation of redox metabolism and to maintain the homeostasis of plant cells, especially in the night.

Discussion

Redox reactions mediated by thioredoxins and thioredoxin reductases are fundamental properties of living cells (Jakupoglu *et al.* 2005; Cheng *et al.* 2017; Biddau *et al.* 2018; Muri *et al.* 2018). For instance, the absence of NADPH-dependent thioredoxin reductase is lethal for mammalian cells (Conrad *et al.* 2004). In contrast to this, neither the lack of the plastidial NADPH-dependent thioredoxin reductase C (NTRC) nor the lack of both non-plastidial NTRA and NTRB is lethal for plant cells (Serrato *et al.* 2004; Reichheld *et al.* 2005). The enhanced robustness of the plant redox network may be associated to their higher number of redundant and compensatory redox players, compared to other organisms (Souza *et al.* 2019). However, it is still not completely understood how the plant NTR system is associated to other redox components, such as the metabolism of ROS, NAD(P)(H), ascorbate and glutathione. This is partially due to the lack of information from plants missing the complete set of NTRs. Here, we characterized the triple *ntrabc* mutant to obtain better insights into the role of NTRs for the regulation of photosynthesis, metabolism and plant growth in different environments as well as to investigate how the complete lack of all NTRs affects plant redox metabolism.

NTR proteins are highly important for photosynthesis and plant growth, but not essential for full Arabidopsis development

We generated an Arabidopsis mutant lacking all NTR isoforms through crossing *ntrab* and *ntrc* mutants. Western blot analysis demonstrated that *ntrabc* plants showed no detectable signals for the NTRA, NTRB and NTRC proteins, indicating a complete knockout in these proteins (Figure S1a). It was previously shown that the *ntrab* and especially the *ntrc* mutant have reduced plant growth, compared to WT (Serrato *et al.* 2004; Reichheld *et al.* 2007; Daloso *et al.* 2015; Thormählen *et al.* 2015; Ojeda *et al.* 2017). We hypothesized that the additional absence of NTRA and NTRB would cause a more severe growth restriction in the *ntrc* background. However, no significant difference in biomass production between *ntrc* and *ntrabc* was observed in plants grown in NC under medium or fluctuating light conditions (Figure 1b). Moreover, while *ntrabc* triple mutant

revealed the same pale green phenotype (Figure 1a), it showed higher Y(II) and lower NPQ than *ntrc* single mutant during dark-light transitions and fluctuating light intensities (Figures 1c-d, S3a-b), indicating increased rather than a decreased photosynthetic performance. Furthermore, no difference in F_v/F_m between the source leaves of WT, *ntrc*, *ntrab* and *ntrabc* plants under NC or HC was observed (Figure 4). Thus, contrary to the expected, the additional lack of NTRA and B did not aggravate the photosynthetic impairment in source leaves caused by NTRC knockout. These results are in line with previous studies showing that extra-plastidial components of the NTR/TRX system (i.e. NTRA, NTRB, TRX *o1* and TRX *h2*) affect photosynthetic efficiency of Arabidopsis plants in an opposing manner than plastidial ones (Reinholdt *et al.* 2019b; Hou *et al.* 2021), when analysed in specific environmental conditions, including FL (Hou et al. 2021) or drought (Fonseca-Pereira *et al.* 2019).

Although the mechanisms by which extra-chloroplastic redox players regulate photosynthetic efficiency are unclear, it has been shown that glycine decarboxylase (GDC), a key photorespiratory enzyme, is deactivated by DTT, NTRA+TRX *o1* and NTRA+TRX *h2 in vitro* (Reinholdt *et al.* 2019b; Fonseca-Pereira *et al.* 2020). Further evidence on the connection between the NTR/TRX system and photorespiration comes from results showing that (i) the rate of oxygen inhibition of photosynthesis was higher in the *trxo1* mutant, when compared to the WT, (ii) the Gly to Ser ratio was higher in the *trxo1* mutant than the WT when transferred from 1500 ppm to 390 ppm of CO_2 concentration, and (iii) the activation of Gly-to-Ser conversion catalysed by GDC and serine hydroxymethyltransferase (SHMT) is slowed down in *trxo1* at onset of illumination (Reinholdt *et al.* 2019b a). These results collectively suggests that the increased photosynthetic efficiency of the triple *ntrabc* mutant, as compared to the *ntrc* mutant, could be associated to higher photorespiratory fluxes during short-term changes in light intensity, as demonstrated for the *trxo1 trxh2* double mutant (Hou *et al.* 2021), which, in turn, would favour the photosynthetic process during dark-to-light transition and under FL condition (Bourguignon *et al.* 1988; Timm *et al.* 2012, 2015). It is noteworthy that such operation might be a short-term effect, only occurring when plants experience a dark-to-light transition or undergo rapid fluctuation in light intensity.

Despite their reduced growth, *ntrabc* plants were able to complete their life cycle and produce fertile seeds (Figure S1b). This demonstrates that NTR proteins are not

essential for full plant development. This is probably due to the complexity of the plant redox network, in which other redundant or compensatory mechanisms overcome, at least to some extent, the complete absence of an important component of the cellular redox system. The absence of NTRC and NTRA/B is likely safeguarded by FTRs and GRs, respectively (Reichheld *et al.* 2007; Marty *et al.* 2009, 2019; Yoshida & Hisabori 2016a). Furthermore, NTRC is a major hub of the plastidial redox network, being directly or indirectly connected to proteins from different redox systems, such as GPX1, tAPX, FTR, GRX, 2-Cys PRX and several TRXs (Souza *et al.* 2019). These results highlight that the presence of numerous redundant and compensatory systems is an important characteristic of plants, which was likely acquired through gene duplication, polyploidization, horizontal gene transfer and/or non-random mutations (Ren *et al.* 2018; Bowles *et al.* 2020; Ma *et al.* 2022; Monroe *et al.* 2022).

The NTR system is crucial for plant acclimation to high CO_2 and for the regulation of sink leaf primary metabolism

Our imaging PAM analysis demonstrated that the potential maximum quantum yield of the PSII (F_v/F_m) is distinctly lower in sink than source leaves of both *ntrc* and *ntrabc* mutants in both NC and HC conditions (Figures 4c-d). Comparing the growth increment of plants grown under HC, in comparison to the NC condition, the *ntrc* mutant showed the lowest plant diameter and leaf-number. Whilst substantial increases in these values were observed in WT and *ntrab* under HC, no difference in both plant diameter and leaf-number in the *ntrabc* was observed in HC, compared to NC (Figures 5e-f). These results provide evidence that plant acclimation to HC is dependent on NTR proteins, especially NTRC. In fact, plant acclimation to HC relies on redox metabolism (Foyer & Noctor 2020), which is likely associated to modifications in the redox status and the metabolism of H_2O_2, glutathione and NAD(P)(H) in different subcellular organelles (Mhamdi & Noctor 2016). Changes in H_2O_2 signalling are rather expected given that HC reduce the peroxisomal turnover of this molecule (Munné-Bosch *et al.* 2013; Sousa *et al.* 2019). Additionally, we demonstrated that the Gly/Ser ratio, a strong indicative of photorespiratory activity (Timm *et al.* 2012), was at least 2.6-fold higher in sink leaves of *ntrc* and *ntrabc* than in source and sink WT leaves under HC condition (Figure S6f). In part, this result is likely associated with GDC activity (Fonseca-Pereira *et al.* 2020),

specifically by the NH_4^+ release by GDC, which in turn may affect the operation of glutamine synthetase (GS)/glutamate synthase (GOGAT) cycle (Wingler *et al.* 2000; Taira *et al.* 2004). This aid to explain the strong increases observed in asparagine (Asn) in sink leaves of both *ntrc* and *ntrabc* plants under HC (Figure 7), given that Asn synthesis through the activity of Asn synthetase involves the transfer of the amide group of glutamine to aspartate, producing Asn and glutamate (Sieciechowicz *et al.* 1988). Asn is an important source of nitrogen for Gly synthesis (Ta *et al.* 1985; Ta & Joy 1986), especially in sink tissues (Kambhampati *et al.* 2017), and its concentration changes according to the photorespiratory flux (Modde *et al.* 2017) or in response to different stress conditions (Lea *et al.* 2007). Therefore, it seems likely that the redox-dependent plant acclimation to HC involves changes in the photorespiratory metabolism and ROS signalling across different subcellular compartments, especially in sink leaves. However, it remains unclear how redox-mediated mechanisms regulate the metabolism of Asn in sink leaves.

Although source leaves are supposedly the major contributors for plant growth, given that sink leaves do not export carbohydrates to other plant organs (Fettke & Fernie 2015), evidence supports the notion that source and sink leaves co-limit plant growth (Jonik *et al.* 2012; Burnett *et al.* 2016; Fernie *et al.* 2020). In this context, our results suggest that the strongly reduced photosynthetic capacity of *ntrc* and *ntrabc* sink leaves greatly contributed to the limited HC acclimation, evidenced by the reductions in rosette diameter and number of leaves in *ntrc* plants under HC, compared to NC (Figure 5f). Although our data does not allow us to fully understand why the lack of NTRC leads to a greater impact in sink leaves, we demonstrated that the concentration of several intermediates from stress-related pathways such as arginine, histidine, branched chain amino acids (Leu, Ile and Val), and Asn is higher in sink than source leaves of both *ntrc* and *ntrabc* (Figure 7). These results, coupled to the lower values of F_v/F_m and 3-PGA and higher Gly/Ser ratio, strongly suggests an imbalance in CO_2/O_2 assimilation by RuBisCO (ribulose-1,5-bisphosphate carboxylase/oxygenase) in sink leaves of *ntrc* and *ntrabc* mutants. These results highlight that NTR proteins, especially NTRC, may have a crucial role for plant acclimation in the current climate change scenario.

The concentration of malate, citrate, fumarate and succinate were substantially altered in both sink and source leaves of the mutants under either NC or HC conditions,

when compared to the WT (Figure 7), which might be related to the role of the NTR/TRX system in the regulation of TCA cycle enzymes (Scheibe & Anderson 1981; Hara *et al.* 2006; Daloso *et al.* 2015; Yoshida & Hisabori 2016b; Huang *et al.* 2017). The intriguingly question remaining is why the effects of NTR absence are more prominent in the metabolism of sink than source leaves. Does the NTR/TRX-mediated metabolic regulation differs between source and sink leaves? Alternatively, the metabolic alterations observed in *ntrc* and *ntrabc* sink leaves are due to an increased level of stress in these leaves. Whilst further experiments are needed to deeply investigate the role of the NTR/TRX system in sink leaves, our imaging PAM and LC-MS-based metabolic analyses clearly demonstrate that the alternative hypothesis holds true. Furthermore, recent evidence highlights that NTRC plays a crucial role for the regulation of carbohydrate and organic acid metabolisms as well as to maintain the NAD(P)(H) redox state of heterotrophic tomato fruits (Hou *et al.* 2021), indicating that the role of NTRC may be wider than those frequently reported for source leaves, and may include sink tissues and non-photosynthetic metabolism (Michalska *et al.* 2009). These results open several avenues to understand the function of NTRs in sink leaves and for the nitrogen remobilization from source to sink leaves and the overall plant growth.

The dark side of redox regulation: the lack of NTRs substantially alters redox metabolism, especially at night

Plant cells have multiple sources of H_2O_2 production and ROS scavenging systems across the cellular organelles (Smirnoff & Arnaud 2019). We showed that *ntrc*, *ntrab* and *ntrabc* mutants have increased leaf H_2O_2 concentration at EN, while no differences among the genotypes were found at ED (Figures 8a, e). Although all NTR mutants showed lower activity of APX and CAT than WT at ED, these differences were more prominent at EN (Figure 8c, d, g, h). Furthermore, the redox status of ASC/DHA and GSH/GSSG of NTR mutants was mainly altered at EN (Figure S9). The most drastic changes observed at EN explain the higher accumulation of H_2O_2 in this period, especially CAT and APX activities and the concentration of GSSG that were negatively and positively correlated with H_2O_2 concentration, respectively (Figure 10b). These results highlight that NTR proteins are important to maintain redox homeostasis of the cell, especially in the night period. The lack of difference in the leaf H_2O_2 content between the

mutants and the WT at ED could be related to redundant or complementary systems that could overcome, at least partially, the lack of NTRs, especially NTRC that has an important role for the chloroplastic metabolism in illuminated leaves (Cejudo *et al.* 2021). Indeed, it has been shown that NTRC acts in cooperation with the FTR system, that is dependent of the ferredoxin produced during photochemical reactions of the chloroplast (Yoshida & Hisabori 2016a). Furthermore, NTRC is highly co-expressed and interacts with other redox components of the chloroplast at gene and protein-protein levels, respectively (Souza *et al.* 2019). This suggests that NTRC is safeguarded by several other redox players in the light, which could have been activated in the mutants to maintain H_2O_2 homeostasis at ED. In the other hand, it has been shown that the non-chloroplastic NTR system is functionally compensated by GRs (Reichheld *et al.* 2007). However, it is unknown to which extent these redox players can compensate the lack of NTRs in the dark-exposed leaves. Thus, neither our data nor previous results could fully explain the overaccumulation of H_2O_2 found here. Although we have measured the activity or the content of important redox-related enzymes/molecules, the phenotype of *ntr* mutants could be further associated to a deregulation of other redox components such as GRs, FTRs, GRXs, GPXs, PRXs, 2-Cys PRXs, and other components of the large plant redox system that acts in the night (Marty *et al.* 2009, 2019; Sousa *et al.* 2015; Yoshida & Hisabori 2016a; Calderón *et al.* 2018).

On the stability of NADP/NADPH and the altered NAD^+/NADH balance in plants lacking NTRs

NAD(H) and NADP(H) are important and intrinsic components of redox metabolism, playing a central role as signalling molecules, energy transducers, cofactors and allosteric regulators of several enzymes of photosynthesis and (photo)respiration (Smith *et al.* 2021). The balance of these pyridine nucleotides is thus of outmost importance to control the metabolic fluxes throughout these pathways by directly (de)activating their enzymes and indirectly by providing reducing power to the NTR/TRX system (Møller *et al.* 2020; Fonseca-Pereira *et al.* 2021). The lack of changes in $NADP^+$ and NADPH concentrations in *ntrc*, *ntrab* and *ntrabc* mutants suggests that NTR proteins are not critical for the regulation of enzymes related to NADPH production under the conditions analysed. Whilst the FTR/TRX system likely compensated the absence of

NTRC to maintain NADPH production via the chloroplastic electron transport chain (cETC) and NADP-dependent MDH (Scheibe & Anderson 1981; Scheibe 1987; Yoshida & Hisabori 2016b; Hashida *et al.* 2018), the synthesis of NADPH by glucose-6-phosphate dehydrogenase (G6PDH) in the cytosol and isocitrate dehydrogenases (IDH) in cytosol and mitochondria may be safeguarded by the GR/GSH/GRX system (Reichheld *et al.* 2007; Marty *et al.* 2009, 2019).

NADH is an allosteric regulator of GDC and several TCA cycle enzymes, beyond being the substrate of the complex I of the mitochondrial ETC (mETC) (Schertl & Braun 2014). Changes in NADH/NAD^+ ratio may thus affect the kinetics of GDC and TCA cycle enzymes, ultimately regulating the metabolic fluxes throughout the (photo)respiratory metabolism (Timm & Hagemann 2020). Here, *ntrabc* plants showed increased NADH concentration and higher and lower proportion (%) of NADH and NAD^+ produced at ED (Figures S7h-S8c). None of these results were found in either *ntrc* or *ntrab* plants, suggesting that a cumulative effect deriving from the lack of all NTRs disrupted NADH/NAD^+ balance at ED. Higher NADH could be related to a higher production from glycolysis and the TCA cycle. This hypothesis is supported by findings in which higher respiratory rate and increased metabolic flux throughout the TCA cycle were observed in mitochondrial NTR/TRX mutants (Daloso *et al.* 2015; Florez-Sarasa *et al.* 2019; Nietzel *et al.* 2020; Lima *et al.* 2021), which might be associated to a light-mediated, negative regulation of fumarase, succinate dehydrogenase and the mitochondrial lipoamide dehydrogenase, that composes different mitochondrial complexes such as GDC, PDH and OGDH, *in vivo* (Daloso *et al.* 2015; Reinholdt *et al.* 2019b). Recent biosensor analysis indicates that light exposure increases the cytosolic NADH/NAD^+ ratio (and likely the NADPH/$NADP^+$ as well) in a process dependent on photosynthesis and chloroplastic and mitochondrial MDHs (Elsässer *et al.* 2020; Steinbeck *et al.* 2020). This highlights the importance of MDHs and the circulating malate for cell redox homeostasis (Souza *et al.* 2019; Zhao *et al.* 2020). Thus, although NTR proteins may represent important sinks for NADPH and NADH consumption *in vivo* (Møller *et al.* 2020), the lack of them is likely compensated by mechanisms that maintain the redox regulation of NAD(P)H-producing enzymes such as GDC, IDHs, MDHs and G6PDH.

Concluding remarks

Our results demonstrate a previously unknown role of NTR proteins to be crucial for the regulation of sink leaf primary metabolism and for plant acclimation to elevated CO_2. While this was mainly associated to the lack of NTRC, the additional lack of NTRA and NTRB was mainly affecting growth and photosynthetic parameters in normal CO_2. Moreover, the triple *ntrabc* showed more drastic changes in redox related parameters compared to WT, *ntrc* and *ntrab*, such as the NADH/NAD^+ balance in the light period and both the activity of ROS-scavenging enzymes and the concentration of GSSG at night. Interestingly, during dark-light transitions and in fluctuating light the *ntrabc* triple mutant displayed improved photosynthetic parameters compared to the *ntrc* single mutant, indicating functional interactions between plastidial and extra-plastidial NTR isoforms during short-term light transients. Overall, our study strengthens the idea that NTR proteins act cooperatively with other redox players, to guarantee the full development of Arabidopsis plants, while they are crucial for optimal functioning of photosynthesis and (photo)respiratory metabolism, especially under high CO_2 concentrations.

Acknowledgments

This work was partially supported by the National Institute of Science and Technology in Plant Physiology under Stress Conditions (INCT Plant Stress Physiology – Grant: 406455/2022-8) and the National Council for Scientific and Technological Development (CNPq, Grant No. 404817/2021-1). DMD thanks the research fellowship granted by CNPq. ARF and PG acknowledge the support of the Deutsche Forschungsgemeinschaft in the framework of the transregional collaborative research centre TRR175. PVLS and HB thank the scholarships granted by the Brazilian Federal Agency for Support and Evaluation of Graduate Education (CAPES). We further thank Dario Leister (LMU Munich) for providing PAM instruments, Anne Bierling (LMU Munich) for maintaining the Arabidopsis mutant lines. We are also grateful to the green house staff of LMU Munich Biocenter for taking care of Arabidopsis plants and MPIMP and MSBioLMU for mass spectrometry analyses. ST thanks Martin Hagemann (Rostock University) for continuous support and HS gratefully acknowledges the scholarship granted by the China Scholarship Council (CSC). JPR, AD and LB are funded by the Centre National de la Recherche

Scientifique, by the National Research Agency (grant nos. ANR-REPHARE 19–CE12–0027 and ANR-RoxRNase 20-CE12-0025) and Labex AGRO (under I-Site Muse framework) coordinated by the Agropolis Fondation (grant no. Flagship Project 1802-002 - CalClim) the LabEx TULIP (ANR-10-LABX-41). AD is supported by a Ph.D. grant from the University of Perpignan Via Domitia (ED305).

Author Contributions

AD, LB and JPR obtained the triple mutant. PVLS, DMD, ST, LYH and PG designed the research. PVLS, LYH, HS, LP, APDJ, HB, AD, LB and ST carried out the analysis, with supervision of JPR, ML, ARF, JAGS, PG or DMD. All authors have contributed to writing and approved the final version of the manuscript.

Conflict of interest

The authors declare no potential conflict of interest.

References

Beers R.F. & Sizer I.W. (1952) A spectrophotometric method for measuring the breakdown of hydrogen peroxide by catalase. *The Journal of biological chemistry* **195**, 133–140.

Biddau M., Bouchut A., Major J., Saveria T., Tottey J., Oka O., … Sheiner L. (2018) Two essential Thioredoxins mediate apicoplast biogenesis, protein import, and gene expression in Toxoplasma gondii. *PLoS Pathogens* **14**, 1–27.

Blanc G., Barakat A., Guyot R., Cooke R. & Delseny M. (2000) Extensive duplication and reshuffling in the Arabidopsis genome. *Plant Cell* **12**, 1093–1101.

Bourguignon J., Neuburger M. & Douce R. (1988) Resolution and characterization of the glycine-cleavage reaction in pea leaf mitochondria. Properties of the forward reaction catalysed by glycine decarboxylase and serine hydroxymethyltransferase. *The Biochemical journal* **255**, 169–178.

Bowles A.M.C., Bechtold U. & Paps J. (2020) The Origin of Land Plants Is Rooted in Two Bursts of Genomic Novelty. *Current Biology* **30**, 530–536.e2.

Boyes D.C., Zayed A.M., Ascenzi R., McCaskill A.J., Hoffman N.E., Davis K.R. & Görlach J. (2001) Growth stage-based phenotypic analysis of Arabidopsis: A model for high throughput functional genomics in plants. *Plant Cell* **13**, 1499–

1510.

Bradford M.M. (1976) A rapid and sensitive method for the quantitation of microgram quantities of protein utilizing the principle of protein-dye binding. *Analytical Biochemistry* **72**, 248–254.

Burnett A.C., Rogers A., Rees M. & Osborne C.P. (2016) Carbon source–sink limitations differ between two species with contrasting growth strategies. *Plant Cell and Environment* **39**, 2460–2472.

Calderón A., Sánchez-Guerrero A., Ortiz-Espín A., Martínez-Alcalá I., Camejo D., Jiménez A. & Sevilla F. (2018) Lack of mitochondrial thioredoxin o1 is compensated by antioxidant components under salinity in Arabidopsis thaliana plants. *Physiologia Plantarum*.

Cejudo F.J., González M.C. & Pérez-Ruiz J.M. (2021) Redox regulation of chloroplast metabolism. *Plant Physiology* **186**, 9–21.

Cheng C., Dong Z., Han X., Wang H., Jiang L., Sun J., … Song H. (2017) Thioredoxin a is essential for motility and contributes to host infection of listeria monocytogenes via redox interactions. *Frontiers in Cellular and Infection Microbiology* **7**, 1–19.

Conrad M., Jakupoglu C., Moreno S.G., Lippl S., Banjac A., Schneider M., … Brielmeier M. (2004) Essential Role for Mitochondrial Thioredoxin Reductase in Hematopoiesis, Heart Development, and Heart Function. *Molecular and Cellular Biology* **24**, 9414–9423.

Daloso D.M., Müller K., Obata T., Florian A., Tohge T., Bottcher A., … Fernie A.R. (2015) Thioredoxin, a master regulator of the tricarboxylic acid cycle in plant mitochondria. *Proceedings of the National Academy of Sciences of the United States of America* **112**, E1392–E1400.

Elsässer M., Feitosa-Araujo E., Lichtenauer S., Wagner S., Fuchs P., Giese J., … Schwarzländer M. (2020) Photosynthetic activity triggers pH and NAD redox signatures across different plant cell compartments. *bioRxiv*, 2020.10.31.363051.

Evans M.C., Buchanan B.B. & Arnon D.I. (1966) A new ferredoxin-dependent carbon reduction cycle in a photosynthetic bacterium. *Proceedings of the National Academy of Sciences of the United States of America* **55**, 928–934.

Fernie A.R., Bachem C.W.B., Helariutta Y., Neuhaus H.E., Prat S., Ruan Y.L., … Sonnewald U. (2020) Synchronization of developmental, molecular and metabolic aspects of source–sink interactions. *Nature Plants* **6**, 55–66.

Fettke J. & Fernie A.R. (2015) Intracellular and cell-to-apoplast compartmentation of carbohydrate metabolism. *Trends in Plant Science* **20**, 490–497.

Florez-Sarasa I., Obata T., Del-Saz N.F., Reichheld J.-P., Meyer E.H., Rodriguez-Concepcion M., … Fernie A.R. (2019) The Lack of Mitochondrial Thioredoxin TRXo1 Affects In Vivo Alternative Oxidase Activity and Carbon Metabolism under Different Light Conditions. *Plant and Cell Physiology* **60**, 2369–2381.

Fonseca-Pereira P., Daloso D.M., Gago J., De Oliveira Silva F.M., Condori-Apfata J.A., Florez-Sarasa I., … Arajo W.L. (2019) The Mitochondrial Thioredoxin System Contributes to the Metabolic Responses under Drought Episodes in Arabidopsis. *Plant and Cell Physiology* **60**, 213–229.

Fonseca-Pereira P., Souza P.V.L., Fernie A.R., Timm S., Daloso D.M. & Araújo W.L. (2021) Thioredoxin-mediated regulation of (photo)respiration and central metabolism. *Journal of Experimental Botany* **72**, 5987–6002.

Fonseca-Pereira P., Souza P.V.L., Hou L.-Y., Schwab S., Geigenberger P., Nunes-Nesi A., … Daloso D.M. (2020) Thioredoxin h2 contributes to the redox regulation of mitochondrial photorespiratory metabolism. *Plant, Cell & Environment* **43**, 188–208.

Foyer C.H., Baker A., Wright M., Sparkes I.A., Mhamdi A., Schippers J.H.M. & Van Breusegem F. (2020) On the move: Redox-dependent protein relocation in plants. *Journal of Experimental Botany* **71**, 620–631.

Foyer C.H. & Noctor G. (2020) Redox Homeostasis and Signaling in a Higher-CO2 World. *Annual Review of Plant Biology* **71**, 157–182.

Geigenberger P., Thormählen I., Daloso D.M. & Fernie A.R. (2017) The Unprecedented Versatility of the Plants Thioredoxin System. *Trends in Plant Science* **22**, 249–262.

Giannopolitis C.N. & Ries S.K. (1977) Superoxide Dismutases: II. Purification and Quantitative Relationship with Water-soluble Protein in Seedlings. *Plant physiology* **59**, 315–318.

Griffith O.W. (1980) Determination of glutathione and glutathione disulfide using glutathione reductase and 2-vinylpyridine. *Analytical Biochemistry* **106**, 207–212.

Hara S., Motohashi K., Arisaka F., Romano P.G.N., Hosoya-Matsuda N., Kikuchi N., … Hisabori T. (2006) Thioredoxin-h1 reduces and reactivates the oxidized cytosolic malate dehydrogenase dimer in higher plants. *Journal of Biological Chemistry* **281**, 32065–32071.

Hashida S., Miyagi A., Nishiyama M., Yoshida K., Hisabori T. & Kawai-Yamada M.

(2018) Ferredoxin/thioredoxin system plays an important role in the chloroplastic <scp>NADP</scp> status of Arabidopsis. *The Plant Journal* **95**, 947–960.

Havir E. a & McHale N. a (1987) Biochemical and developmental characterization of multiple forms of catalase in tobacco leaves. *Plant physiology* **84**, 450–455.

Hendriks J.H.M., Kolbe A., Gibon Y., Stitt M. & Geigenberger P. (2003) ADP-Glucose Pyrophosphorylase Is Activated by Posttranslational Redox-Modification in Response to Light and to Sugars in Leaves of Arabidopsis and Other Plant Species. *Plant Physiology* **133**, 838–849.

Hou L.-Y., Lehmann M. & Geigenberger P. (2021) Thioredoxin h2 and o1 Show Different Subcellular Localizations and Redox-Active Functions, and Are Extrachloroplastic Factors Influencing Photosynthetic Performance in Fluctuating Light. *Antioxidants* **10**, 705.

Huang J., Niazi A.K., Young D., Rosado L.A., Vertommen D., Bodra N., … Reichheld J.-P. (2017) Self-protection of cytosolic malate dehydrogenase against oxidative stress in Arabidopsis. *Journal of Experimental Botany* **69**, 3491–3505.

Jakupoglu C., Przemeck G.K.H., Schneider M., Moreno S.G., Mayr N., Hatzopoulos A.K., … Conrad M. (2005) Cytoplasmic Thioredoxin Reductase Is Essential for Embryogenesis but Dispensable for Cardiac Development. *Molecular and Cellular Biology* **25**, 1980–1988.

Jonik C., Sonnewald U., Hajirezaei M.R., Flügge U.I. & Ludewig F. (2012) Simultaneous boosting of source and sink capacities doubles tuber starch yield of potato plants. *Plant Biotechnology Journal* **10**, 1088–1098.

Kambhampati S., Ajewole E. & Marsolais F. (2017) Advances in Asparagine Metabolism. In *Progress in Botany*. pp. 49–74.

Kampfenkel K., Van Montagu M. & Inzé D. (1995) Extraction and determination of ascorbate and dehydroascorbate from plant tissue. *Analytical Biochemistry* **225**, 165–167.

Kopka J., Schauer N., Krueger S., Birkemeyer C., Usadel B., Bergmüller E., … Steinhauser D. (2005) GMD@CSB.DB: The Golm metabolome database. *Bioinformatics* **21**, 1635–1638.

Laloi C., Rayapuram N., Chartier Y., Grienenberger J.-M., Bonnard G. & Meyer Y. (2001) Identification and characterization of a mitochondrial thioredoxin system in plants. *Proceedings of the National Academy of Sciences* **98**, 14144–14149.

Lampl N., Lev R., Nissan I., Gilad G., Hipsch M. & Rosenwasser S. (2022) Systematic

monitoring of 2-Cys peroxiredoxin-derived redox signals unveiled its role in attenuating carbon assimilation rate. *Proceedings of the National Academy of Sciences of the United States of America* **119**, 1–10.

Lea P.J., Sodek L., Parry M.A.J., Shewry P.R. & Halford N.G. (2007) Asparagine in plants. *Annals of Applied Biology* **150**, 1–26.

Lima V.F., Erban A., Daubermann A.G., Freire F.B.S., Porto N.P., Cândido-Sobrinho S.A., … Daloso D.M. (2021) Establishment of a GC-MS-based 13C-positional isotopomer approach suitable for investigating metabolic fluxes in plant primary metabolism. *The Plant Journal* **108**, 1213–1233.

Lintala M., Schuck N., Thormählen I., Jungfer A., Weber K.L., Weber A.P.M., … Mulo P. (2014) Arabidopsis tic62 trol Mutant Lacking Thylakoid-Bound Ferredoxin–NADP+ Oxidoreductase Shows Distinct Metabolic Phenotype. *Molecular Plant* **7**, 45–57.

Lisec J., Schauer N., Kopka J., Willmitzer L. & Fernie A.R. (2006) Gas chromatography mass spectrometry-based metabolite profiling in plants. *Nature Protocols* **1**, 387–396.

López-Grueso M.J., González-Ojeda R., Requejo-Aguilar R., McDonagh B., Fuentes-Almagro C.A., Muntané J., … Padilla C.A. (2019) Thioredoxin and glutaredoxin regulate metabolism through different multiplex thiol switches. *Redox Biology* **21**, 101049.

Luedemann A., Strassburg K., Erban A. & Kopka J. (2008) TagFinder for the quantitative analysis of gas metabolite profiling experiments. *Bioinformatics* **24**, 732–737.

Ma J., Wang S., Zhu X., Sun G., Chang G., Li L., … Huang J. (2022) Major episodes of horizontal gene transfer drove the evolution of land plants. *Molecular Plant* **15**, 857–871.

Martí M.C., Jiménez A. & Sevilla F. (2020) Thioredoxin Network in Plant Mitochondria: Cysteine S-Posttranslational Modifications and Stress Conditions. *Frontiers in Plant Science* **11**, 1–20.

Marty L., Bausewein D., Müller C., Bangash S.A.K., Moseler A., Schwarzländer M., … Meyer A.J. (2019) Arabidopsis glutathione reductase 2 is indispensable in plastids, while mitochondrial glutathione is safeguarded by additional reduction and transport systems. *New Phytologist* **224**, 1569–1584.

Marty L., Siala W., Schwarzlander M., Fricker M.D., Wirtz M., Sweetlove L.J., … Hell

R. (2009) The NADPH-dependent thioredoxin system constitutes a functional backup for cytosolic glutathione reductase in Arabidopsis. *Proceedings of the National Academy of Sciences* **106**, 9109–9114.

Meyer A.J., Dreyer A., Ugalde J.M., Feitosa-Araujo E., Dietz K.J. & Schwarzländer M. (2021) Shifting paradigms and novel players in Cys-based redox regulation and ROS signaling in plants - And where to go next. *Biological Chemistry* **402**, 399–423.

Meyer Y., Buchanan B.B., Vignols F. & Reichheld J.-P. (2009) Thioredoxins and Glutaredoxins: Unifying Elements in Redox Biology. *Annual Review of Genetics* **43**, 335–367.

Mhamdi A. & Noctor G. (2016) High CO2 primes plant biotic stress defences through redox-linked pathways. *Plant Physiology* **172**, 929–942.

Michalska J., Zauber H., Buchanan B.B., Cejudo F.J. & Geigenberger P. (2009) NTRC links built-in thioredoxin to light and sucrose in regulating starch synthesis in chloroplasts and amyloplasts. *Proceedings of the National Academy of Sciences of the United States of America* **106**, 9908–9913.

Modde K., Timm S., Florian A., Michl K., Fernie A.R. & Bauwe H. (2017) High serine:glyoxylate aminotransferase activity lowers leaf daytime serine levels, inducing the phosphoserine pathway in Arabidopsis. *Journal of Experimental Botany* **68**, 643–656.

Møller I.M., Igamberdiev A.U., Bykova N. V., Finkemeier I., Rasmusson A.G. & Schwarzländer M. (2020) Matrix redox physiology governs the regulation of plant mitochondrial metabolism through posttranslational protein modifications. *Plant Cell* **32**, 573–594.

Monroe J.G., Srikant T., Carbonell-Bejerano P., Becker C., Lensink M., Exposito-Alonso M., … Weigel D. (2022) Mutation bias reflects natural selection in Arabidopsis thaliana. *Nature* **602**, 101–105.

Munné-Bosch S., Queval G. & Foyer C.H. (2013) The impact of global change factors on redox signaling underpinning stress tolerance. *Plant Physiology* **161**, 5–19.

Muri J., Heer S., Matsushita M., Pohlmeier L., Tortola L., Fuhrer T., … Kopf M. (2018) The thioredoxin-1 system is essential for fueling DNA synthesis during T-cell metabolic reprogramming and proliferation. *Nature Communications* **9**, 1–16.

Nakano Y. & Asada K. (1981) Hydrogen peroxide is scavenged by ascorbate-specific peroxidase in spinach chloroplasts. *Plant Cell Physiology* **22**, 867–880.

Nietzel T., Mostertz J., Ruberti C., Née G., Fuchs P., Wagner S., … Schwarzländer M. (2020) Redox-mediated kick-start of mitochondrial energy metabolism drives resource-efficient seed germination. *Proceedings of the National Academy of Sciences of the United States of America* **117**, 741–751.

Ojeda V., Pérez-Ruiz J.M., González M., Nájera V.A., Sahrawy M., Serrato A.J., … Cejudo F.J. (2017) NADPH Thioredoxin Reductase C and Thioredoxins Act Concertedly in Seedling Development. *Plant Physiology* **174**, 1436–1448.

Pang Z., Chong J., Zhou G., De Lima Morais D.A., Chang L., Barrette M., … Xia J. (2021) MetaboAnalyst 5.0: Narrowing the gap between raw spectra and functional insights. *Nucleic Acids Research* **49**, W388–W396.

Reichheld J.-P., Khafif M., Riondet C., Droux M., Bonnard G. & Meyer Y. (2007) Inactivation of Thioredoxin Reductases Reveals a Complex Interplay between Thioredoxin and Glutathione Pathways in *Arabidopsis* Development. *The Plant Cell* **19**, 1851–1865.

Reichheld J.P., Meyer E., Khafif M., Bonnard G. & Meyer Y. (2005) AtNTRB is the major mitochondrial thioredoxin reductase in Arabidopsis thaliana. *FEBS Letters* **579**, 337–342.

Reinholdt O., Bauwe H., Hagemann M. & Timm S. (2019a) Redox-regulation of mitochondrial metabolism through thioredoxin o1 facilitates light induction of photosynthesis. *Plant Signaling & Behavior* **14**, 1674607.

Reinholdt O., Schwab S., Zhang Y., Reichheld J.P., Fernie A.R., Hagemann M. & Timm S. (2019b) Redox-regulation of photorespiration through mitochondrial thioredoxin O1. *Plant Physiology* **181**, 442–457.

Ren R., Wang H., Guo C., Zhang N., Zeng L., Chen Y., … Qi J. (2018) Widespread Whole Genome Duplications Contribute to Genome Complexity and Species Diversity in Angiosperms. *Molecular Plant* **11**, 414–428.

Scheibe R. (1987) NADP+-malate dehydrogenase in C3-plants: Regulation and role of a light-activated enzyme. *Physiologia Plantarum* **71**, 393–400.

Scheibe R. & Anderson L.E. (1981) Dark Modulation of Nadp-Dependent Malate Dehydrogenase and Glucose-6-Phosphate. *Biochimica et Biophysica Acta* **636**, 58–64.

Schertl P. & Braun H.P. (2014) Respiratory electron transfer pathways in plant mitochondria. *Frontiers in Plant Science* **5**, 1–11.

Serrato A.J., Pérez-Ruiz J.M., Spínola M.C. & Cejudo F.J. (2004) A novel NADPH

thioredoxin reductase, localised in the chloroplast, which deficiency causes hypersensitivity to abiotic stress in Arabidopsis thaliana. *Journal of Biological Chemistry* **279**, 43821–43827.

Sharkey T.D. (2016) What gas exchange data can tell us about photosynthesis. *Plant Cell and Environment* **39**, 1161–1163.

Sieciechowicz K.A., Joy K.W. & Ireland R.J. (1988) The metabolism of asparagine in plants. *Phytochemistry* **27**, 663–671.

Smirnoff N. & Arnaud D. (2019) Hydrogen peroxide metabolism and functions in plants. *New Phytologist* **221**, 1197–1214.

Smith E.N., Schwarzländer M., Ratcliffe R.G. & Kruger N.J. (2021) Shining a light on NAD- and NADP-based metabolism in plants. *Trends in Plant Science* **26**, 1072–1086.

Sousa R.H.V., Carvalho F.E.L., Lima-Melo Y., Alencar V.T.C.B., Daloso D.M., Margis-Pinheiro M., … Silveira J.A.G. (2019) Impairment of peroxisomal APX and CAT activities increases protection of photosynthesis under oxidative stress. *Journal of Experimental Botany* **70**, 627–639.

Sousa R.H.V., Carvalho F.E.L., Ribeiro C.W., Passaia G., Cunha J.R., Lima-Melo Y., … Silveira J.A.G. (2015) Peroxisomal APX knockdown triggers antioxidant mechanisms favourable for coping with high photorespiratory H2O2 induced by CAT deficiency in rice. *Plant Cell and Environment* **38**, 499–513.

Souza P.V.L., Lima-Melo Y., Carvalho F.E., Reichheld J.P., Fernie A.R., Silveira J.A.G. & Daloso D.M. (2019) Function and Compensatory Mechanisms Among the Components of the Chloroplastic Redox Network. *Critical Reviews in Plant Sciences* **38**, 1–28.

Steinbeck J., Fuchs P., Negroni Y.L., Elsässer M., Lichtenauer S., Stockdreher Y., … Schwarzländer M. (2020) In vivo nadh/nad1 biosensing reveals the dynamics of cytosolic redox metabolism in plants. *Plant Cell* **32**, 3324–3345.

Ta T.C. & Joy K.W. (1986) Metabolism of some amino acids in relation to the photorespiratory nitrogen cycle of pea leaves. *Planta* **169**, 117–122.

Ta T.C., Joy K.W. & Ireland R. (1985) Role of asparagine in the photochemistry nitrogen metaboliem of pea leaves. *Plant Physiology* **78**, 334–337.

Taira M., Valtersson U., Burkhardt B. & Ludwig R.A. (2004) Arabidopsis thaliana GLN2-encoded glutamine synthetase is dual targeted to leaf mitochondria and chloroplasts. *Plant Cell* **16**, 2048–2058.

Thormählen I., Meitzel T., Groysman J., Öchsner A.B., Von Roepenack-Lahaye E., Naranjo B., … Geigenberger P. (2015) Thioredoxin f1 and NADPH-dependent thioredoxin reductase C have overlapping functions in regulating photosynthetic metabolism and plant growth in response to varying light conditions. *Plant Physiology* **169**, 1766–1786.

Thormählen I., Zupok A., Rescher J., Leger J., Weissenberger S., Groysman J., … Geigenberger P. (2017) Thioredoxins Play a Crucial Role in Dynamic Acclimation of Photosynthesis in Fluctuating Light. *Molecular Plant* **10**, 168–182.

Timm S. & Bauwe H. (2013) The variety of photorespiratory phenotypes – employing the current status for future research directions on photorespiration. **15**, 737–747.

Timm S., Florian A., Arrivault S., Stitt M., Fernie A.R. & Bauwe H. (2012) Glycine decarboxylase controls photosynthesis and plant growth. *FEBS Letters* **586**, 3692–3697.

Timm S. & Hagemann M. (2020) Photorespiration – how is it regulated and regulates overall plant metabolism? *Journal of Experimental Botany*.

Timm S., Wittmiß M., Gamlien S., Ewald R., Florian A., Frank M., … Bauwe H. (2015) Mitochondrial Dihydrolipoyl Dehydrogenase Activity Shapes Photosynthesis and Photorespiration of *Arabidopsis thaliana*. *The Plant Cell* **27**, 1968–1984.

Ugalde J.M., Fuchs P., Nietzel T., Cutolo E.A., Homagk M., Vothknecht U.C., … Meyer A.J. (2021) Chloroplast-derived photo-oxidative stress causes changes in H2O2 and EGSH in other subcellular compartments. *Plant Physiology* **186**, 125–141.

Wingler A., Lea P.J., Quick W.P., Leegood R.C., Trans P., Lond R.S., … Leegood R.C. (2000) Photorespiration : metabolic pathways and their role in stress protection Photorespiration : metabolic pathways and their role in stress protection. 1517–1529.

Yoshida K. & Hisabori T. (2016a) Two distinct redox cascades cooperatively regulate chloroplast functions and sustain plant viability. *Proceedings of the National Academy of Sciences* **113**, E3967–E3976.

Yoshida K. & Hisabori T. (2016b) Adenine nucleotide-dependent and redox-independent control of mitochondrial malate dehydrogenase activity in Arabidopsis thaliana. *Biochimica et Biophysica Acta - Bioenergetics* **1857**, 810–818.

Zhao Y., Yu H., Zhou J.M., Smith S.M. & Li J. (2020) Malate Circulation: Linking Chloroplast Metabolism to Mitochondrial ROS. *Trends in Plant Science* **25**, 446–454.

Zhou M., Diwu Z., Panchuk-voloshina N. & Haugland R.P. (1997) A Stable Nonfluorescent Derivative of Resorufin for the Fluorometric Determination of Trace Hydrogen Peroxide : Applications in Detecting the Activity of Phagocyte NADPH Oxidase and Other Oxidases. **168**, 162–168.

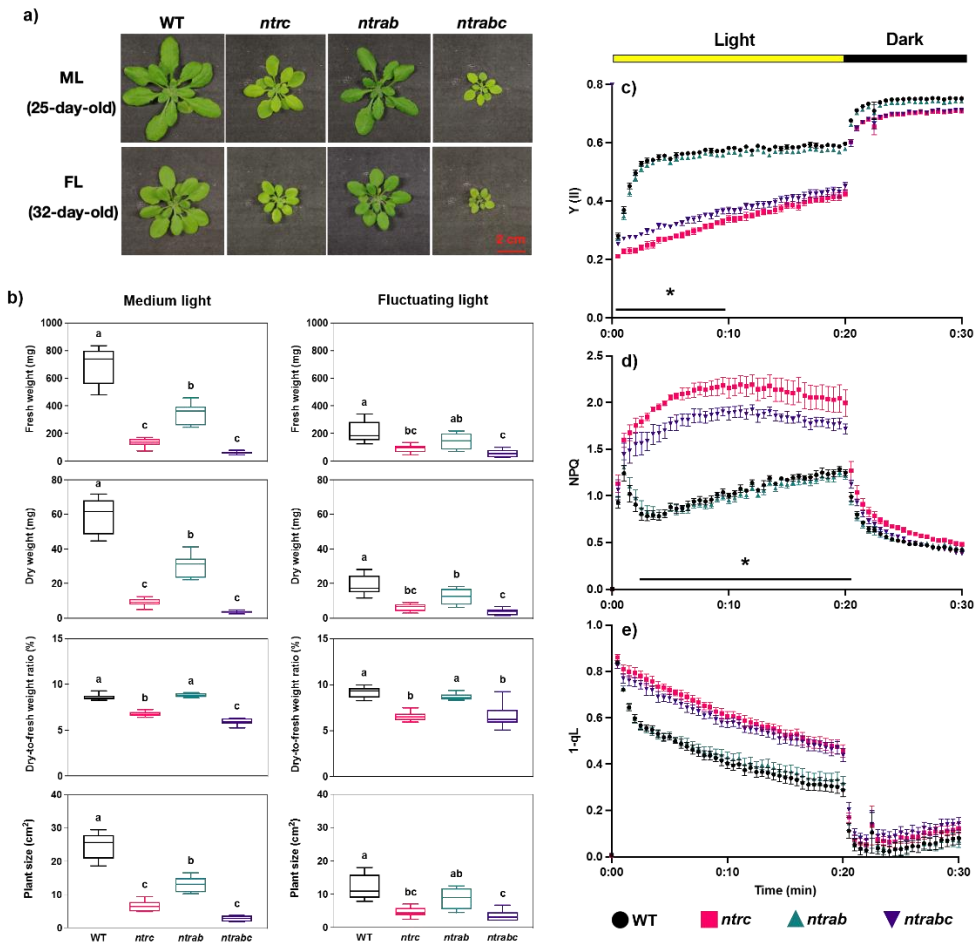

Figure 1 Growth and photosynthetic phenotype of *Arabidopsis thaliana* L. wild type (WT) and mutants lacking NTRC (*ntrc*), NTRA and NTRB (*ntrab*) or all NTRs (*ntrabc*). a) Representative photographs of 25-day-old and 32-day-old Arabidopsis rosettes grown under medium light (ML) or fluctuating light (FL) conditions, respectively. The setup of ML corresponds to ~120 µmol photons m^{-2} s^{-1} (12/12 h photoperiod), while FL represents a loop of low light (50 µmol photons m^{-2} s^{-1} for 5 min) and high light (550 µmol photons $m^{-2}s^{-1}$ for 1 min) phases with the same photoperiod as ML. b) Growth-related parameters determined in WT and NTR mutants grown under ML (left graphs) or FL (right graphs) conditions. After 25 and 35 days under ML or FL conditions, plants were harvested and the fresh weight (FW), dry weight (DW), plant size and the DW-to-FW ratio were determined. Black, pink, green and purple box plots represent averages and standard errors of WT, *ntrc*, *ntrab*, and *ntrabc* genotypes, respectively. Means that do not share a letter are significantly different according to ANOVA and Tukey test analysis ($P < 0.05$) (n = 6 ± SE). c-e) Chlorophyll *a* fluorescence analysis. Effective quantum yield of PSII (Y(II)) (c), non-photochemical quenching (NPQ) (d) and the reduction of plastoquinone pool (1-qL) (e) were measured in WT and NTR mutants grown under ~120 µmol photons m^{-2} s^{-1} (12/12 h photoperiod). Dark-adapted leaves were transferred to the image PAM instrument (MAXI version, WALZ) and subjected to constant light (150 µmol photons m^{-2} s^{-1}) for 20 min (yellow bars), followed by 10 min in the dark (black bars). The emission of chlorophyll *a* florescence was recorded by the image PAM instrument every 30 seconds and used for the calculation of Y(II), 1-qL and NPQ. Asterisks indicate time points in which Y(II) and NPQ are statistically different between *ntrc* and *ntrabc* plants by ANOVA and Tukey test ($P < 0.05$) (n = 6).

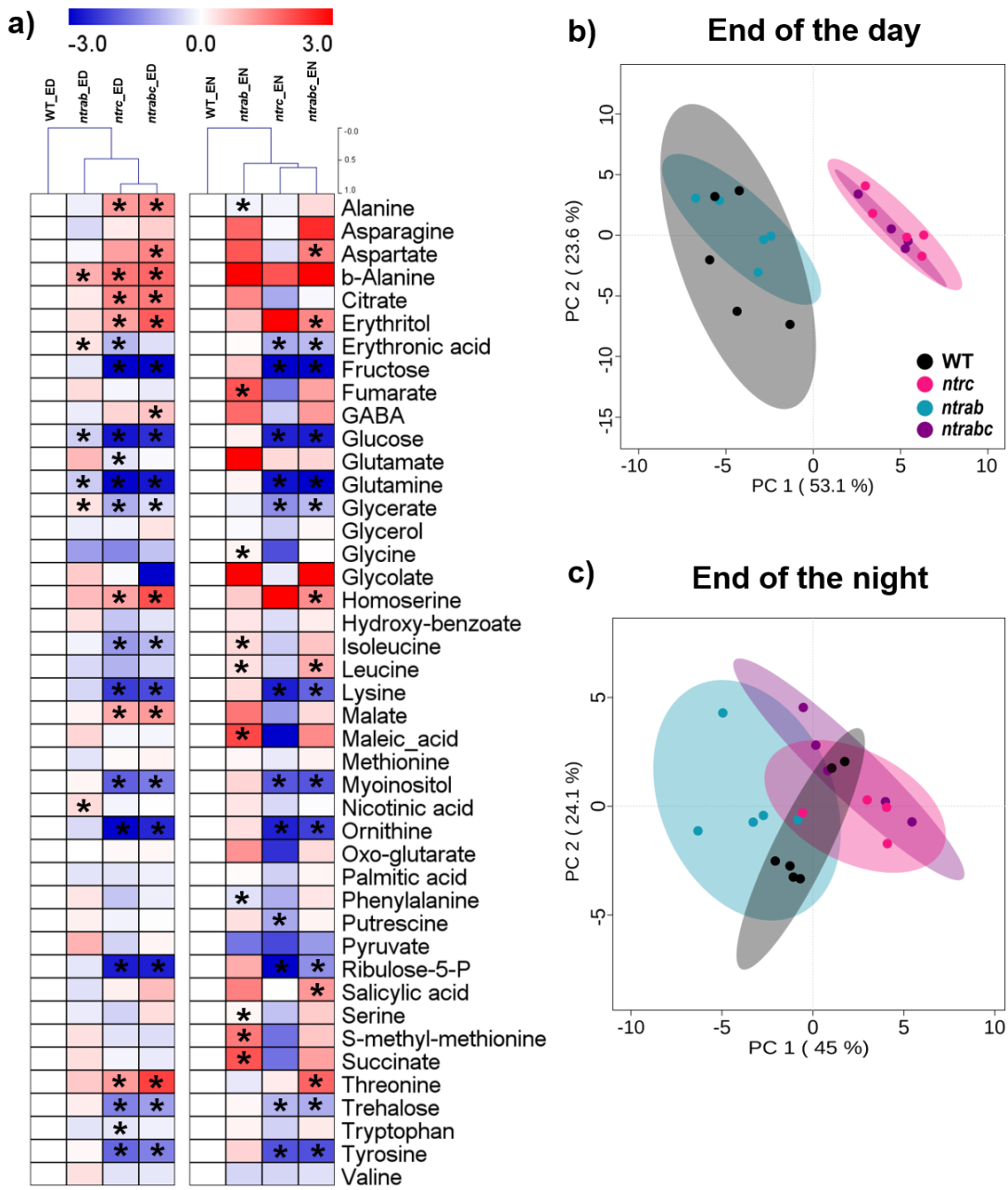

Figure 2 Changes in the metabolite profiling of *Arabidopsis thaliana* L. wild type (WT) and mutants lacking NTRC (*ntrc*), NTRA and NTRB (*ntrab*) or all NTRs (*ntrabc*). a) Heat map representation of the changes in the relative abundance of primary metabolites identified by gas chromatography mass spectrometry (GC-MS) in leaf samples harvested at the end of the day (ED) and the end of the night (EN) of short-day (~120 µmol photons m^{-2} s^{-1}; 08/16 h photoperiod) grown plants. The average values of the relative abundance (normalized to Ribitol and fresh weight) were normalized according to the WT values found at ED and EN and log_2 transformed (n = 4). Asterisks (*) indicate values that are significantly different from the WT by the Student's t-test ($P < 0.05$). b-c) Principal component analysis (PCA) carried out using GC-MS-based metabolite profiling data of WT, *ntrc*, *ntrab*, *ntrabc* harvest at ED (b) or EN (c). The two main components and the percentage variation explained by PC1 and PC2 are represented in the axis of the figures. Heat map and PCA were carried out using MeV and the Metaboanalyst platform, respectively.

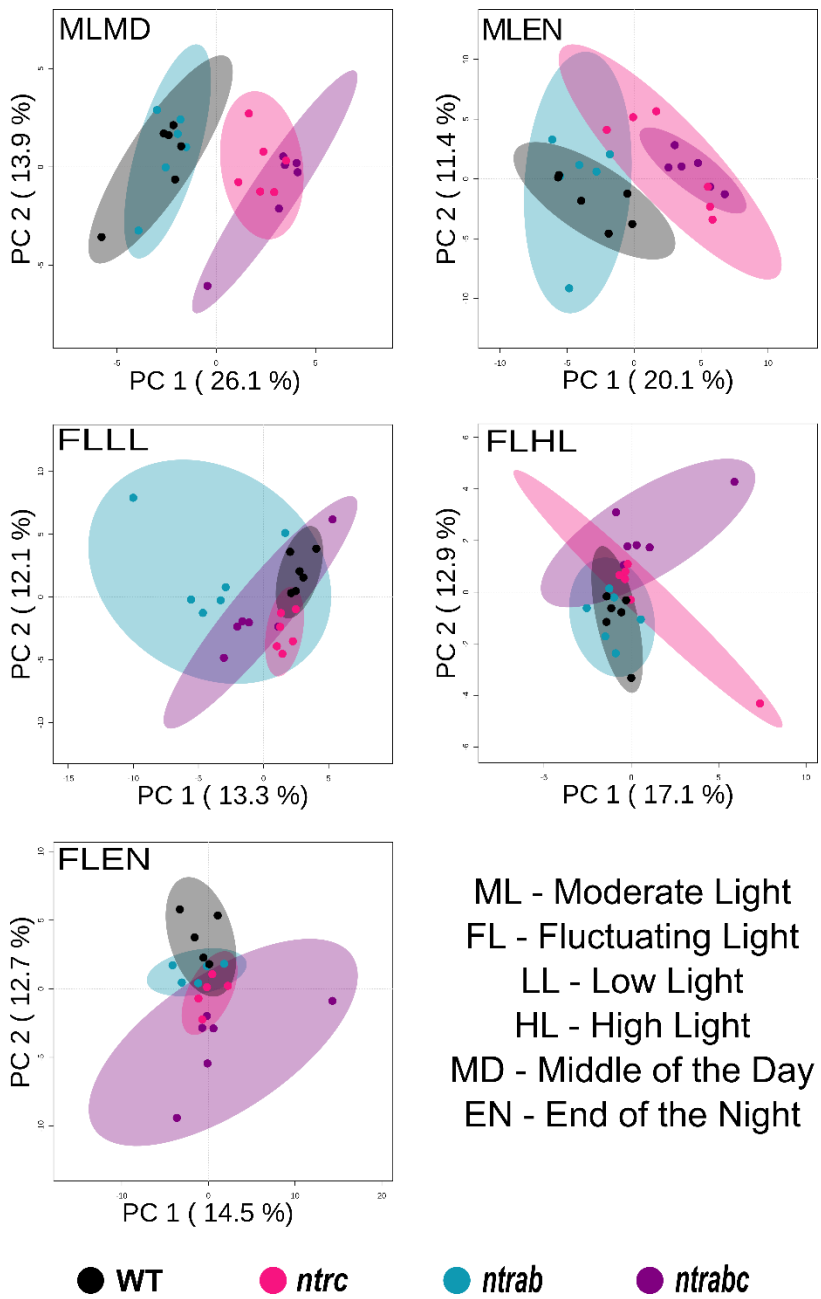

Figure 3 Principal component analysis (PCA) of the metabolite profiling data from *Arabidopsis thaliana* L. wild type (WT) and mutants lacking NTRC (*ntrc*), NTRA and NTRB (*ntrab*) or all NTRs (*ntrabc*). PCA was carried out using leaf GC-MS-based metabolite profiling data of WT, *ntrc*, *ntrab* and *ntrabc* plants grown under medium light (ML) (~120 µmol photons m^{-2} s^{-1}, 12h/12h day/night photoperiod) and after transferred to fluctuating light (FL) conditions (1 minute of high light (HL): 500 µmol photons m^{-2} s^{-1} followed by 5 minutes of low light (LL): 50 µmol photons m^{-2} s^{-1}). After 4 weeks under ML, leaves were harvested at the mid of the day (MLMD) and at the end of the night (MLEN). Plants acclimated to FL were first grown for 3 weeks under ML conditions and then acclimated to 1 week of FL. After that, leaves were harvested at the low light (FLLL) and high light (FLHL) phases of the FL and at EN (FLEN). The percentage variation explained by PC1 and PC2 are represented in the axis of the figures. PCA was carried out using the Metaboanalyst platform.

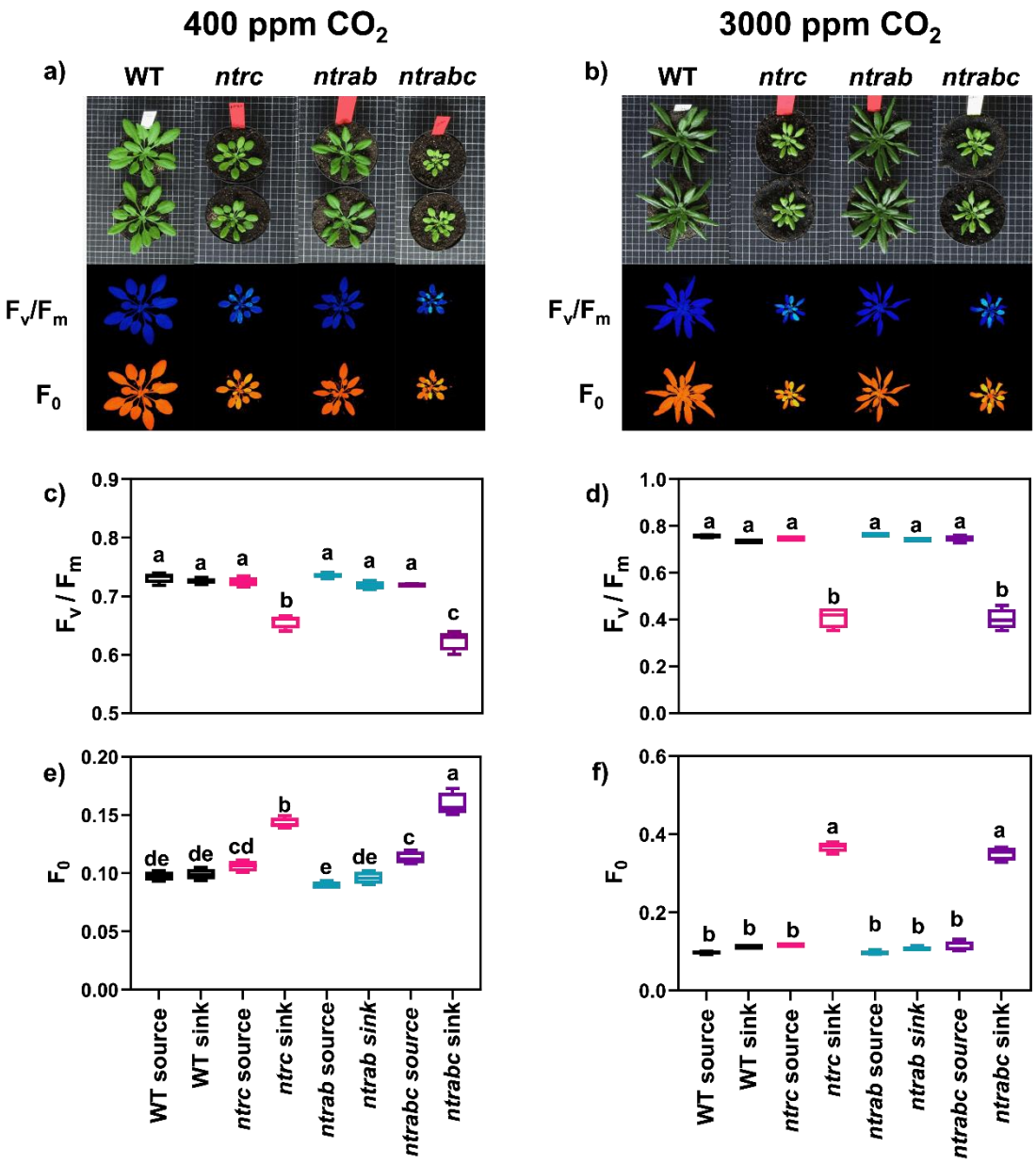

Figure 4 Chlorophyll *a* fluorescence analysis of *Arabidopsis thaliana* L. wild type (WT) and mutants lacking NTRC (*ntrc*), the double NTRA and NTRB (*ntrab*), and the triple NTRs (*ntrabc*). These analyses were carried out on 5-week-old plants grown under ~120 µmol photons m^{-2} s^{-1}, 12/12 h photoperiod and either ambient (NC, 400 ppm) or high (HC, 3000 ppm) CO_2 concentrations. a-b) Representative Arabidopsis rosette images highlighting the size, the potential quantum yield of the photosystem II (F_v/F_m) and the higher minimal fluorescence of dark-adapted leaves (F_0) of WT, *ntrc*, *ntrab*, and *ntrabc* plants under NC (a) or HC (b) conditions. c-f) Box plots representing averages and standard errors of F_v/F_m and F_0 of source and sink leaves from plants grown under NC (c,e) or HC (d,f) conditions. Black, pink, green, and purple colours represent WT, *ntrc*, *ntrab*, and *ntrabc* genotypes, respectively. Means that do not share a letter are significantly different according to ANOVA and Tukey test analysis ($P < 0.05$) (n = 4).

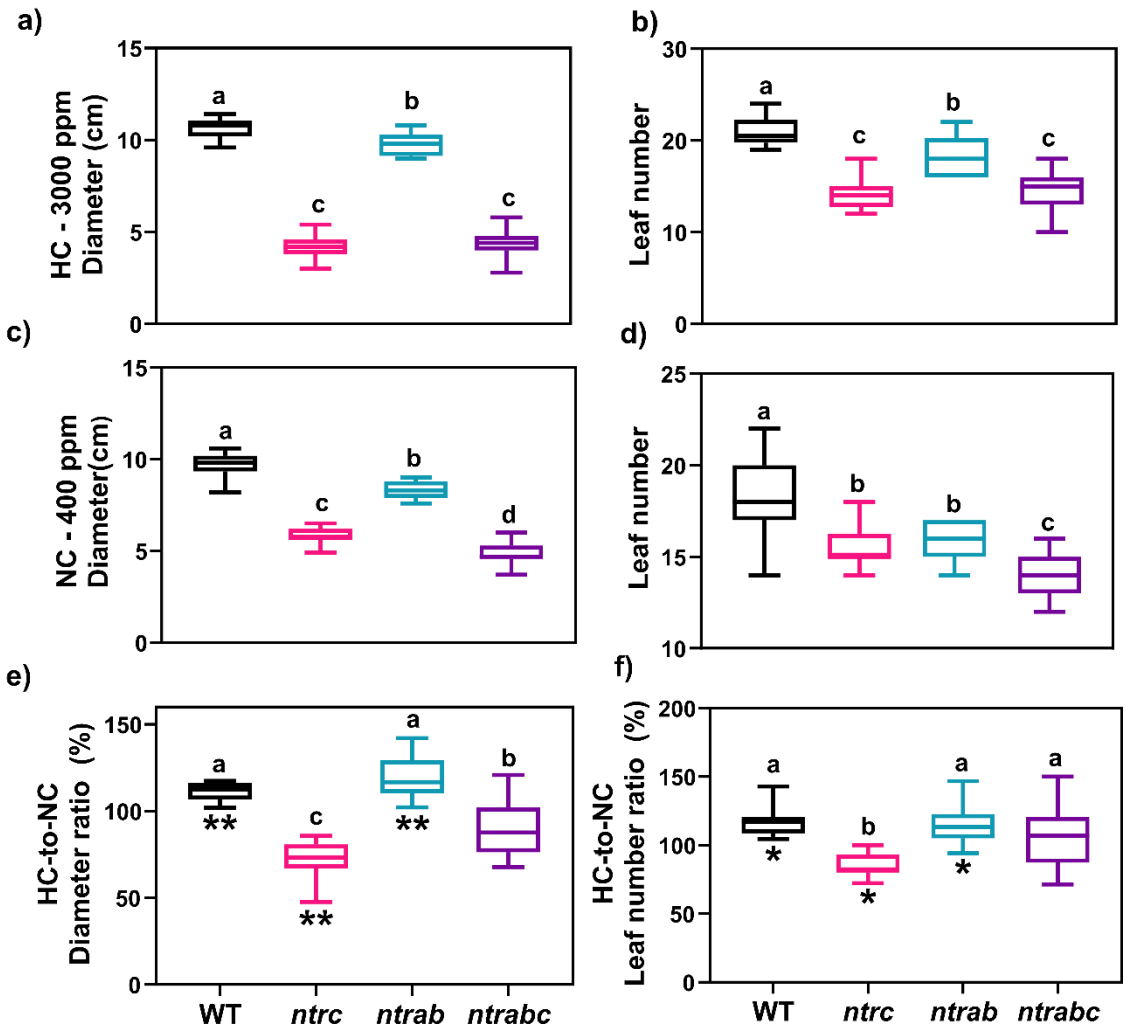

Figure 5 Growth-related parameters determined in *Arabidopsis thaliana* L. wild type (WT) and mutants lacking in NTRC (*ntrc)*, NTRA and NTRB (*ntra* and *ntrb*), and in all NTRs isoforms (*ntrabc*) grown under ambient (NC, 400 ppm) or high (HC, 3000 ppm) CO_2 concentration. The rosette diameter and the number of leaves were determined in plants grown under HC (a-b) and NC (c-d) conditions. The relative changes in these parameters in HC related to NC (HC-to-NC ratio) was also quantified (e-f). Means that do not share a letter are significantly different according to ANOVA and Tukey test analysis ($P < 0.05$). One (*) and two (**) asterisks indicate statistical difference between HC and NC within the genotype at 5% ($P < 0.05$) and 1% ($P < 0.05$) of probability, respectively (n = 6 ± SE).

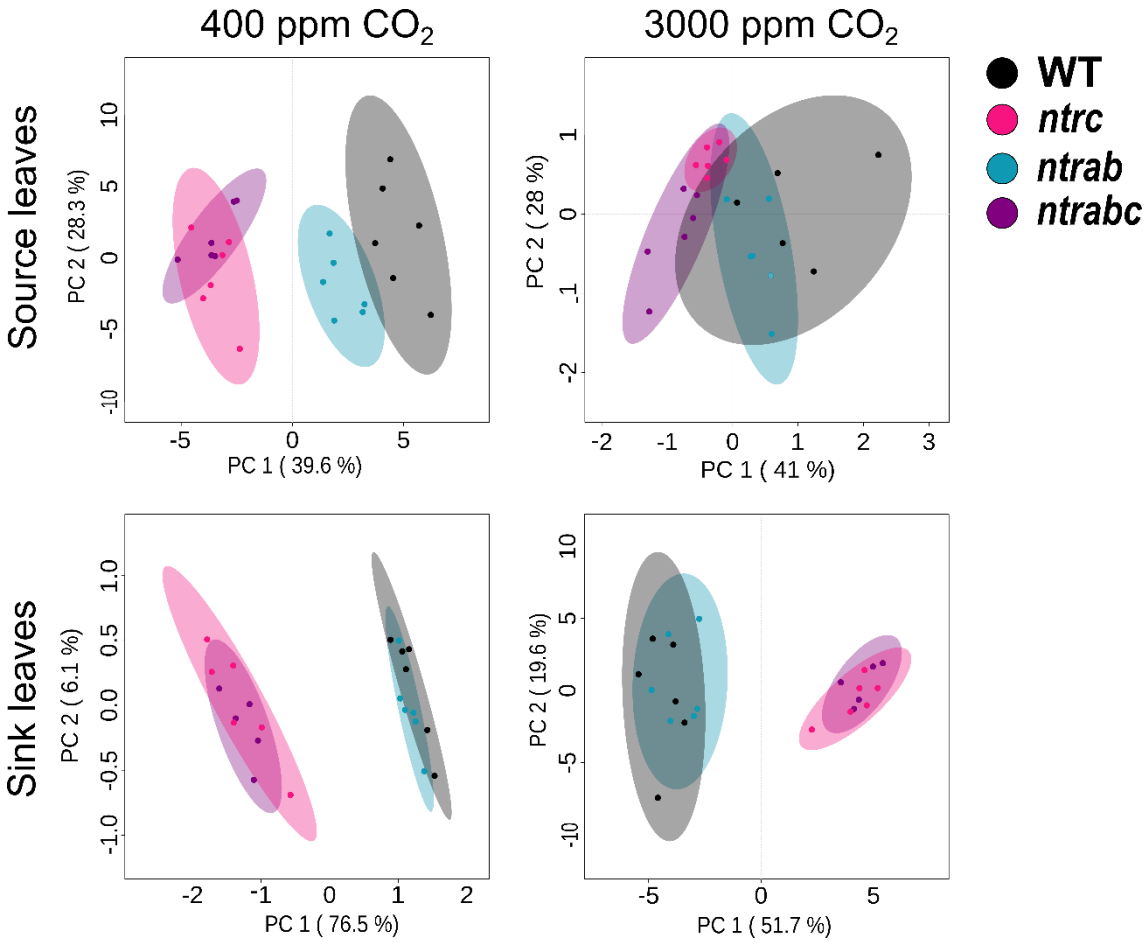

Figure 6 Principal component analysis (PCA) using LC-MS/MS-based metabolite profiling data from source and sink leaves of 5-week-old *Arabidopsis thaliana* L. wild type (WT) and mutants lacking NTRC (*ntrc*), NTRA and NTRB (*ntrab*) or all NTRs (*ntrabc*) grown under ~120 µmol photons m^{-2} s^{-1}, 12/12 h photoperiod and either ambient (NC, 400 ppm) or high (HC, 3000 ppm) CO_2 concentration (n = 5). The two main components and the percentage variation explained by them are represented in the axis of the figures. PCA was carried out using the Metaboanalyst platform.

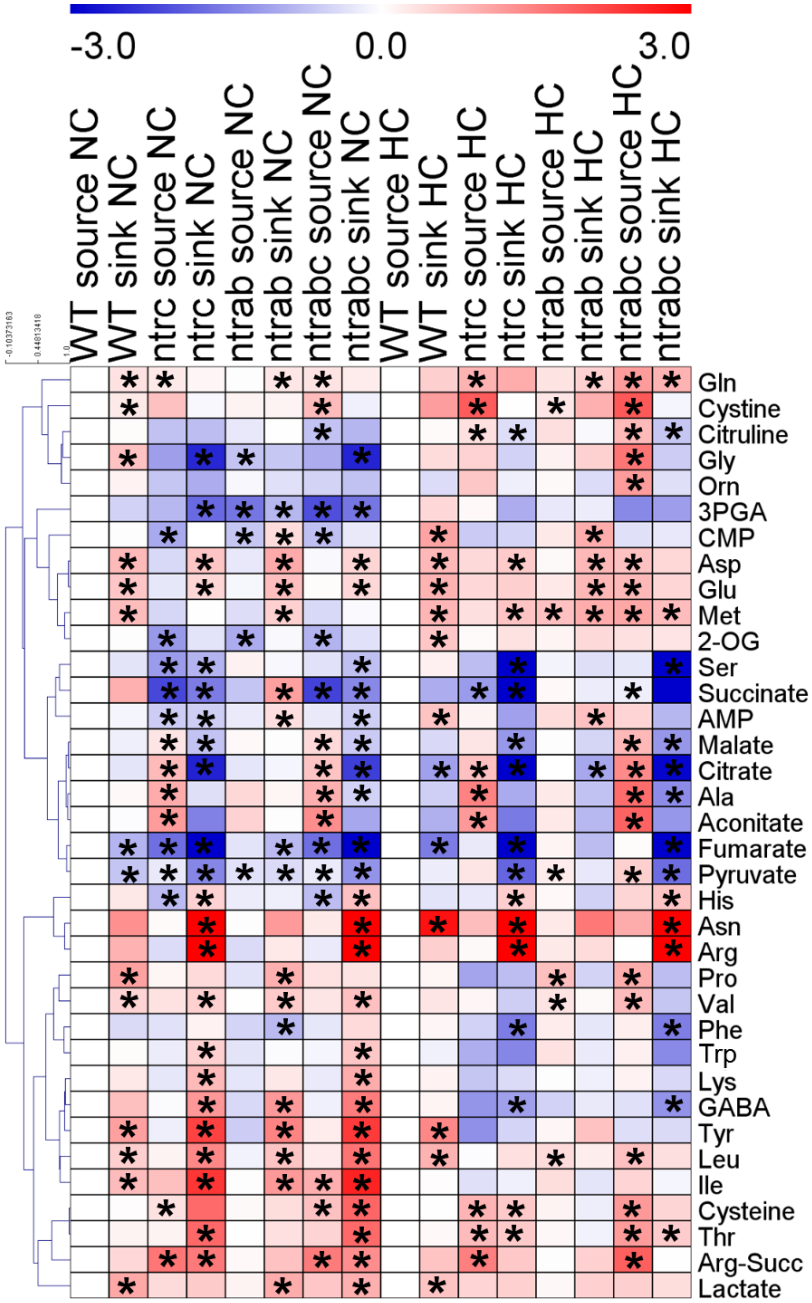

Figure 7 Heat map representation of the concentration of the metabolites of identified in source and sink leaves of 5-week-old *Arabidopsis thaliana* L. wild type (WT) and mutants lacking NTRC (*ntrc*), NTRA and NTRB (*ntrab*) or all NTRs (*ntrabc*) grown under ~120 µmol photons m^{-2} s^{-1}, 12/12 h photoperiod and either ambient (NC, 400 ppm) or high (HC, 3000 ppm) CO_2 concentration. Metabolites were identified by liquid chromatography mass spectrometry (LC-MS/MS) in source and sink leaf samples harvested at the end of the day. The average values of the concentration of the metabolites (ng mg^{-1} FW) were normalized according to the WT values found at NC or HC condition and log_2 transformed. Citrate represents the sum between citrate and isocitrate, that could not be separated by LC-MS/MS. Asterisks (*) indicate values that are significantly different from WT source leaves at NC or HC condition by ANOVA and Dunnet test ($P < 0.05$). Abbreviations of the metabolites are found in the Table S2.

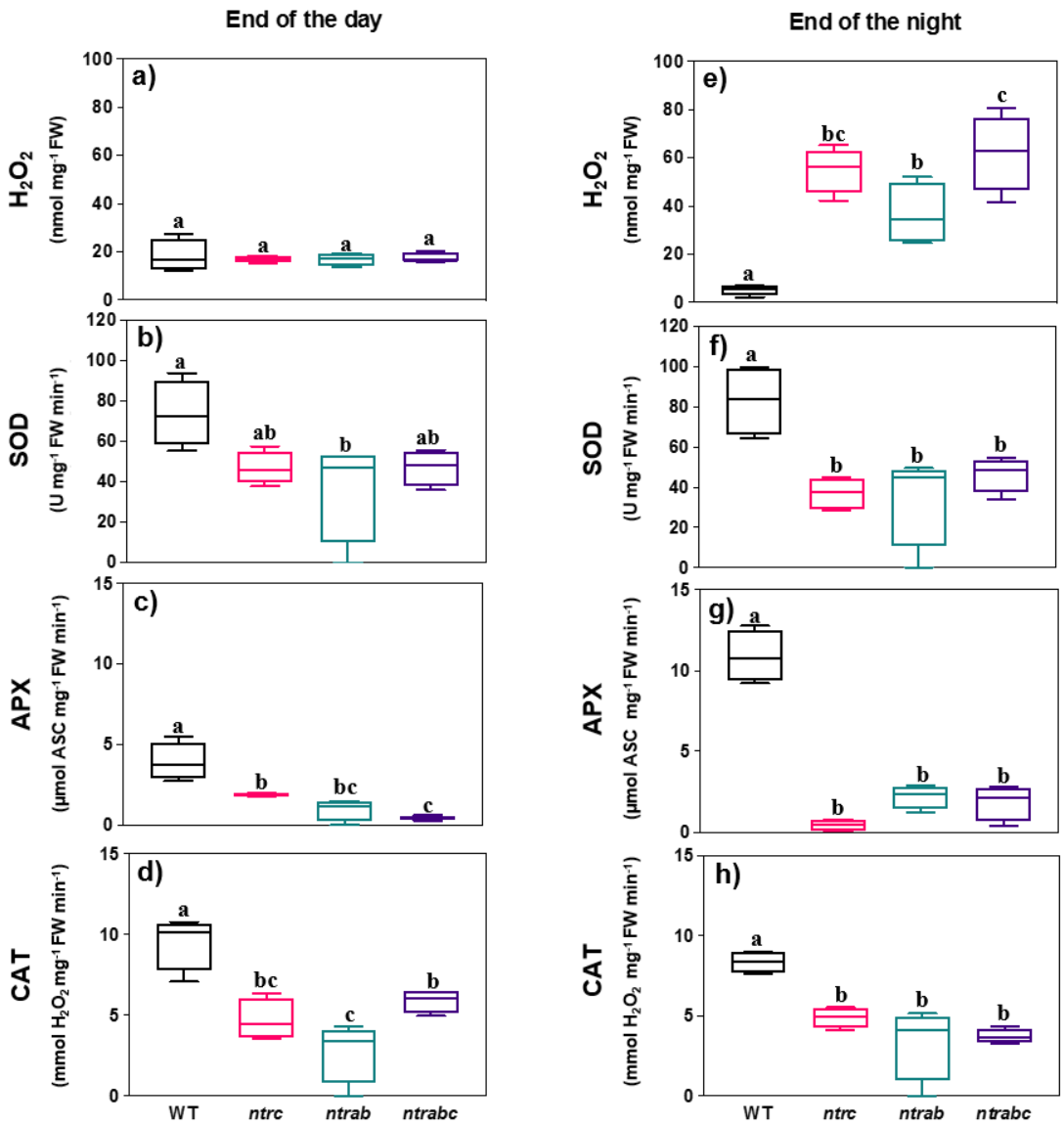

Figure 8 H_2O_2 concentration and activity of antioxidant enzymes in leaves of *Arabidopsis thaliana* L. wild type (WT) and mutants lacking NTRC (*ntrc*), NTRA and NTRB (*ntrab*) or all NTRs (*ntrabc*) harvested at end of the day (ED) (a-d) and end of the night (EN) (e-h) of short-day (~120 µmol photons m^{-2} s^{-1}; 08/16 h photoperiod) grown plants. The concentration of H_2O_2 and the activities of superoxide dismutase (SOD), ascorbate peroxidase (APX) and catalase (CAT) are expressed in a fresh weight (FW) basis. Black, pink, green and purple box plots represent averages and standard errors of WT, *ntrc*, *ntrab*, and *ntrabc* genotypes, respectively (n = 4). Means that do not share a letter are significantly different according to ANOVA and Tukey test analysis ($P < 0.05$).

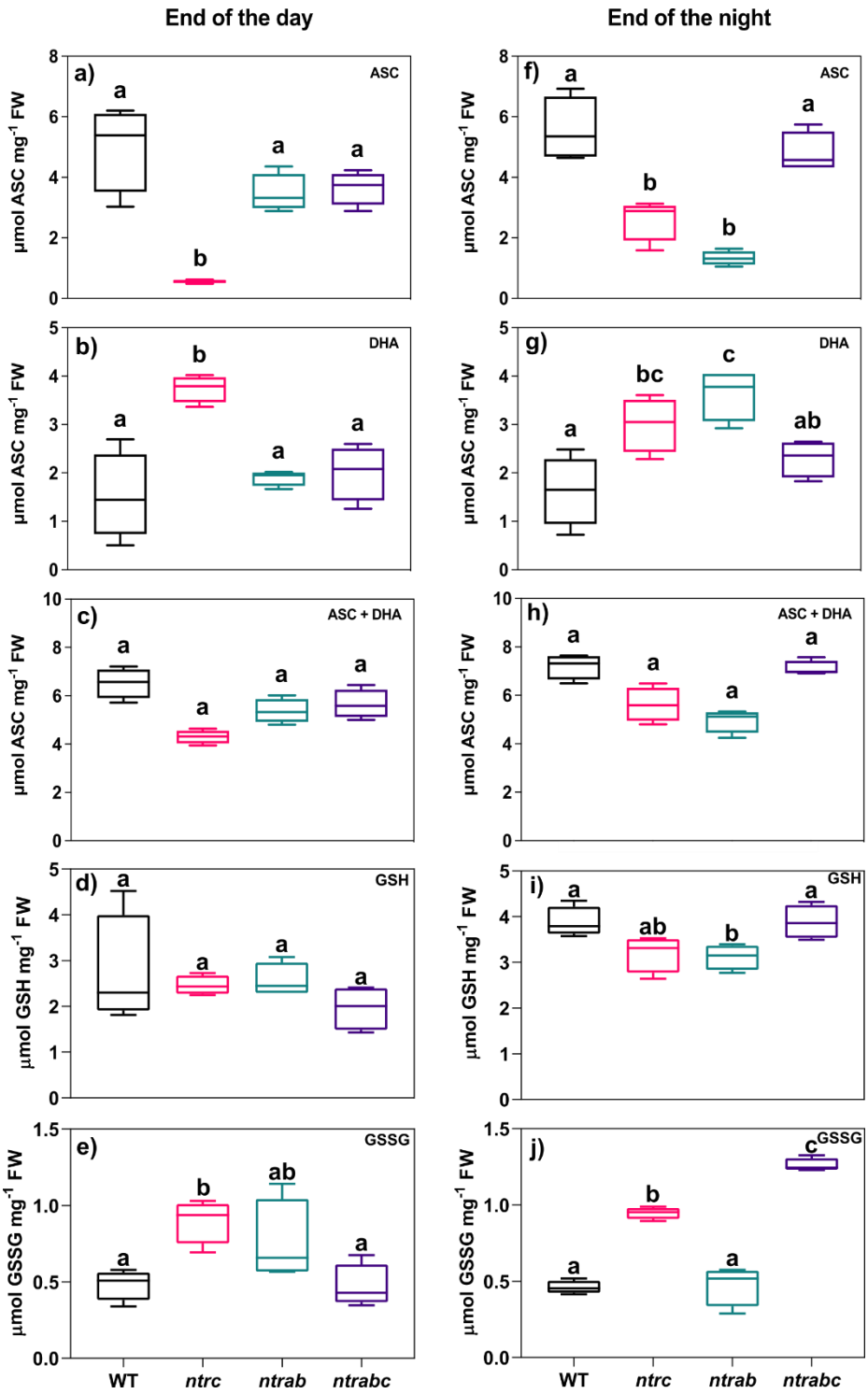

Figure 9 Concentration of ascorbate (ASC), dehydroascorbate (DHA), the sum of them (ASC + DHA), and reduced (GSH) and oxidized (GSSG) glutathione in leaves of *Arabidopsis thaliana* L. wild type (WT) and mutants lacking NTRC (*ntrc*), NTRA and NTRB (*ntrab*) or all NTRs (*ntrabc*) harvested at end of the day (ED) (left panel) and end of the night (EN) (right panel) of short-day (~120 µmol photons m^{-2} s^{-1}; 08/16 h photoperiod) grown plants. Black, pink, green and purple box plots represent averages and standard errors of WT, *ntrc*, *ntrab*, and *ntrabc* genotypes, respectively (n = 4). Means that do not share a letter are significantly different according to ANOVA and Tukey test analysis ($P < 0.05$).

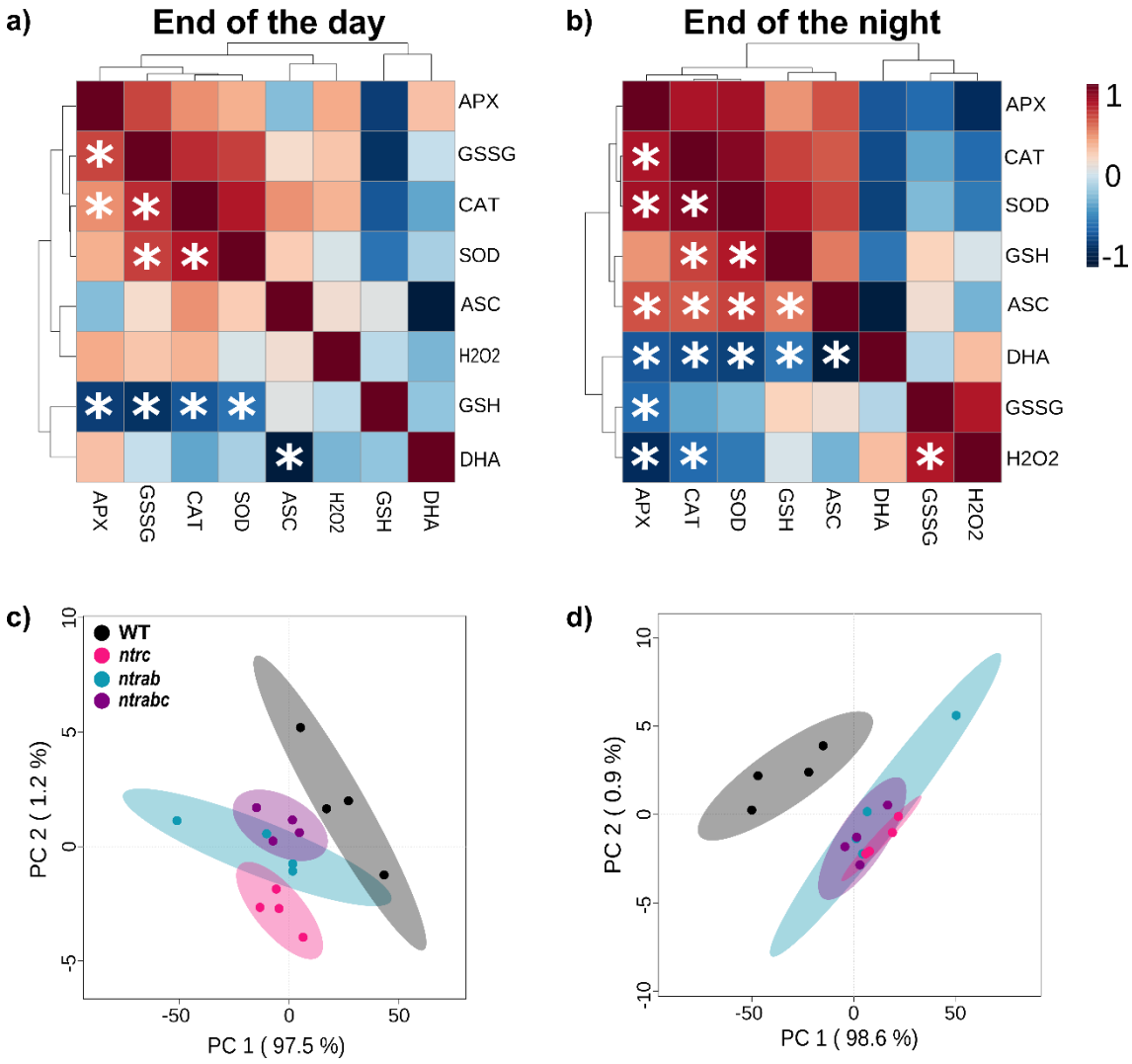

Figure 10 Integrative redox analyses. a-b) Heat map representation of Pearson's correlation analysis between H_2O_2 and components of the antioxidant system. The correlation analysis was carried out using data from all genotypes at end of the day (ED) (left figure) and end of the night (EN) (right figure). Plants were grown under short-day conditions (~120 µmol photons m^{-2} s^{-1}; 08/16 h photoperiod). Asterisks (*) indicate significant correlations ($P < 0.05$). c-d) Principal component analysis (PCA) carried out using redox-related parameters (H_2O_2, ASC, DHA, ASC+DHA, ASC (%), DHA (%), GSH, GSSG, GSH+GSSG, GSH (%), GSSG (%), SOD, CAT, APX) observed in leaves of *Arabidopsis thaliana* L. wild type (WT) and mutants lacking NTRC (*ntrc*), NTRA and NTRB (*ntrab*) or all NTRs (*ntrabc*) harvested at end of the day (c) and end of the night (d) of short-day (~120 µmol photons m^{-2} s^{-1}; 08/16 h photoperiod) grown plants. The two main components and the percentage variation explained by them are represented in the axis of the figures. Both analyses were carried out using the Metaboanalyst platform. Abbreviations: H_2O_2, hydrogen peroxide; ASC, ascorbate; APX, ascorbate peroxidase; CAT, catalase; DHA, dehydroascorbate; GSH, reduced glutathione; GSSG, oxidized glutathione; SOD, superoxide dismutase.

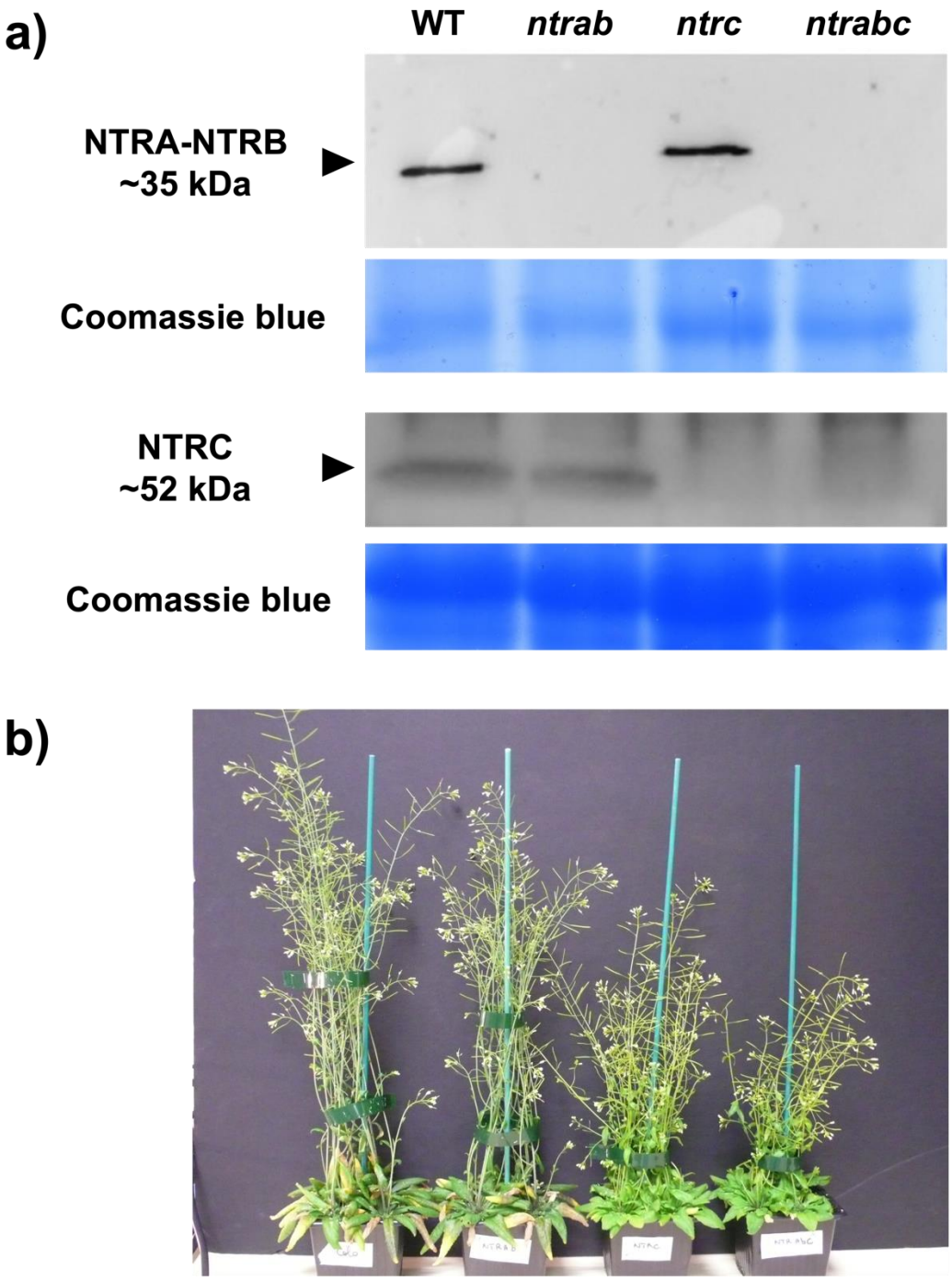

Figure S1 Immunoblot analysis and phenotype of the plants at the reproductive stage. a) Immunoblot detection of NTRC and NTRA/NTRB proteins was carried out in plant extracts of two-week-old *Arabidopsis thaliana* L. wild type (WT) and mutants lacking NTRC (*ntrc*), NTRA and NTRB (*ntrab*) or all NTRs (*ntrabc*). Proteins were separated by SDS-PAGE (10% polyacrylamide) under reducing conditions, then transferred to a nitrocellulose membrane, and incubated with NTRA/NTRB and NTRC antibodies (dilution 1:10.000), followed by incubation with secondary antibody (Sigma secondary antibody anti-rabbit, dilution 1:10,000). The blots were then revealed with enhanced chemiluminescence reagents. b) Phenotype of 49-day old WT, *ntrab*, *ntrc* and *ntrabc* plants grown under 16:8 h photoperiod, highlighting that all mutants were able to complete their life cycle, from vegetative to the reproductive stage.

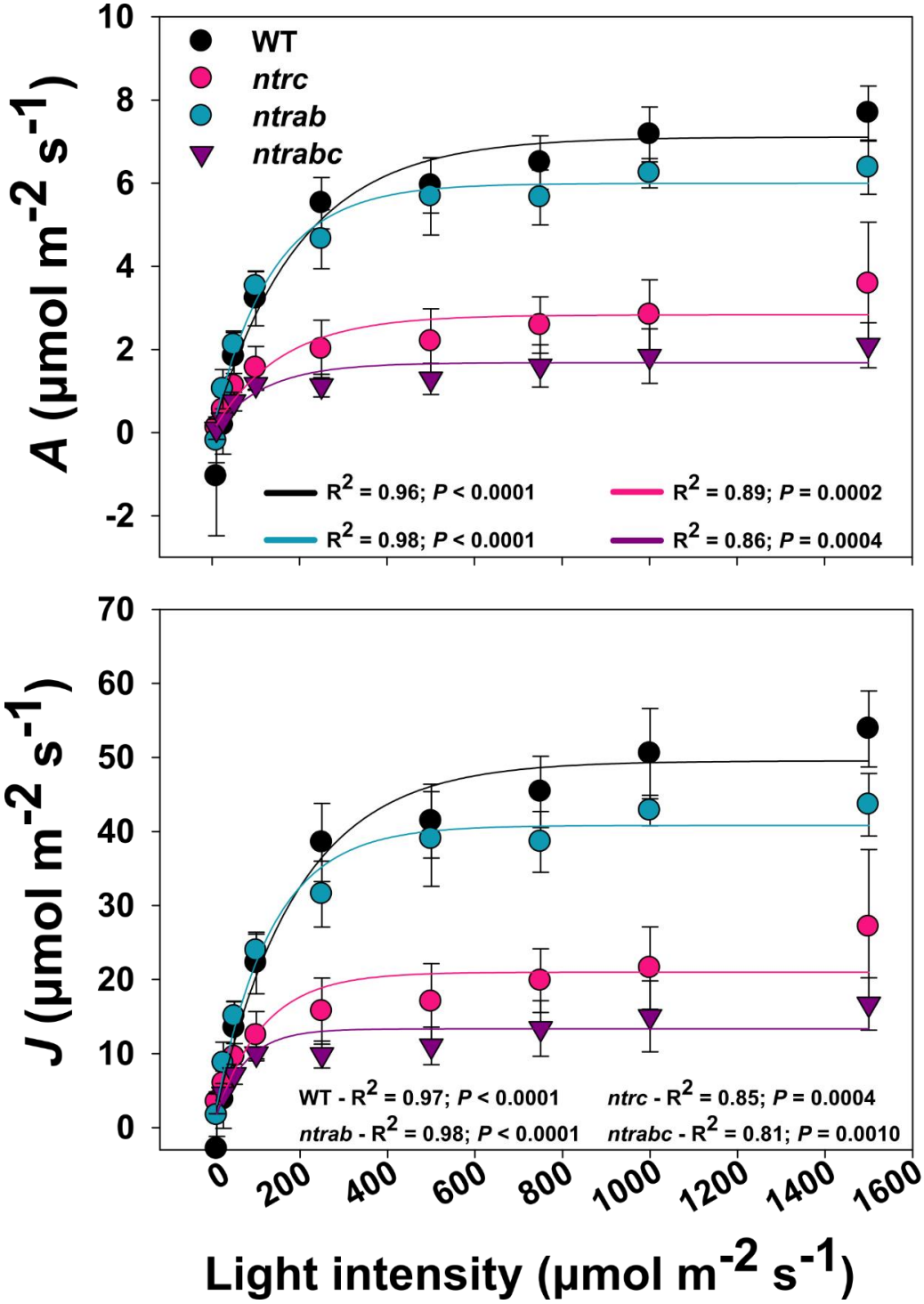

Figure S2 Photosynthetic responses to changes in light intensity. Net CO_2 assimilation (*A*) (a) and maximum electron transport rate (*J*) (b) were obtained from fully expanded leaves of 8-week-old *Arabidopsis thaliana* L. wild type (WT) and mutants lacking NTRC (*ntrc*), NTRA and NTRB (*ntrab*) or all NTRs (*ntrabc*) under different light intensities. This analysis was carried out using a portable infra-red gas exchange analyser. The regression lines were obtained using the equation $Y = a\,(1 - e^{-bx})$, where Y represents *A* and *J* parameters. The values of R^2 and *P* of each regression analysis are highlighted in the graphs (n = 6 ± SD).

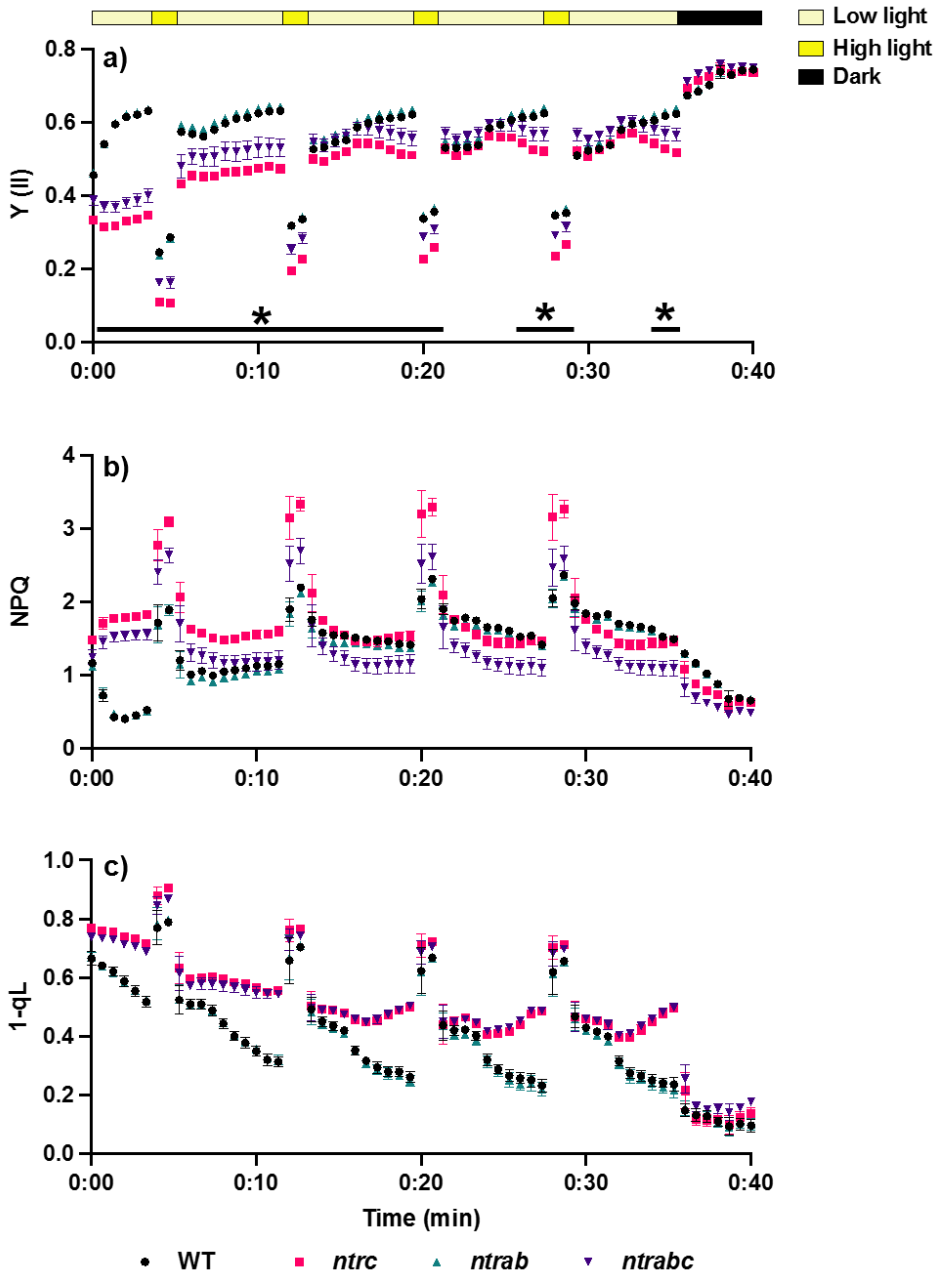

Figure S3 Chlorophyll *a* fluorescence analysis in *Arabidopsis thaliana* L. wild type (WT) and mutants lacking NTRC (*ntrc*), NTRA and NTRB (*ntrab*) or all NTRs (*ntrabc*). Effective quantum yield of PSII (Y(II)) (a), the reduction of plastoquinone pool (1-qL) (b) and non-photochemical quenching (NPQ) (c) were measured in WT and NTR mutants grown under fluctuating light regime (5 min of 50 µmol photons m^{-2} s^{-1} 1 min of 550 µmol photons $m^{-2}s^{-1}$, 12:12 h photoperiod). Dark-adapted leaves were transferred to the image PAM instrument (MAXI version, WALZ) and subjected to low light (50 µmol photons $m^{-2}s^{-1}$) followed by 4 cycles of FL comprising 1 min high light (500 µmol photons $m^{-2}s^{-1}$) and 6 min low light (50 µmol photons $m^{-2}s^{-1}$), and then the dark for another 5 min. The emission of chlorophyll *a* florescence was recorded by the image PAM instrument every 30 seconds and used for the calculation of Y(II), 1-qL and NPQ. Asterisks indicate time points in which Y(II) and NPQ are statistically different between *ntrc* and *ntrabc* plants by ANOVA and Tukey test ($P < 0.05$) (n = 6).

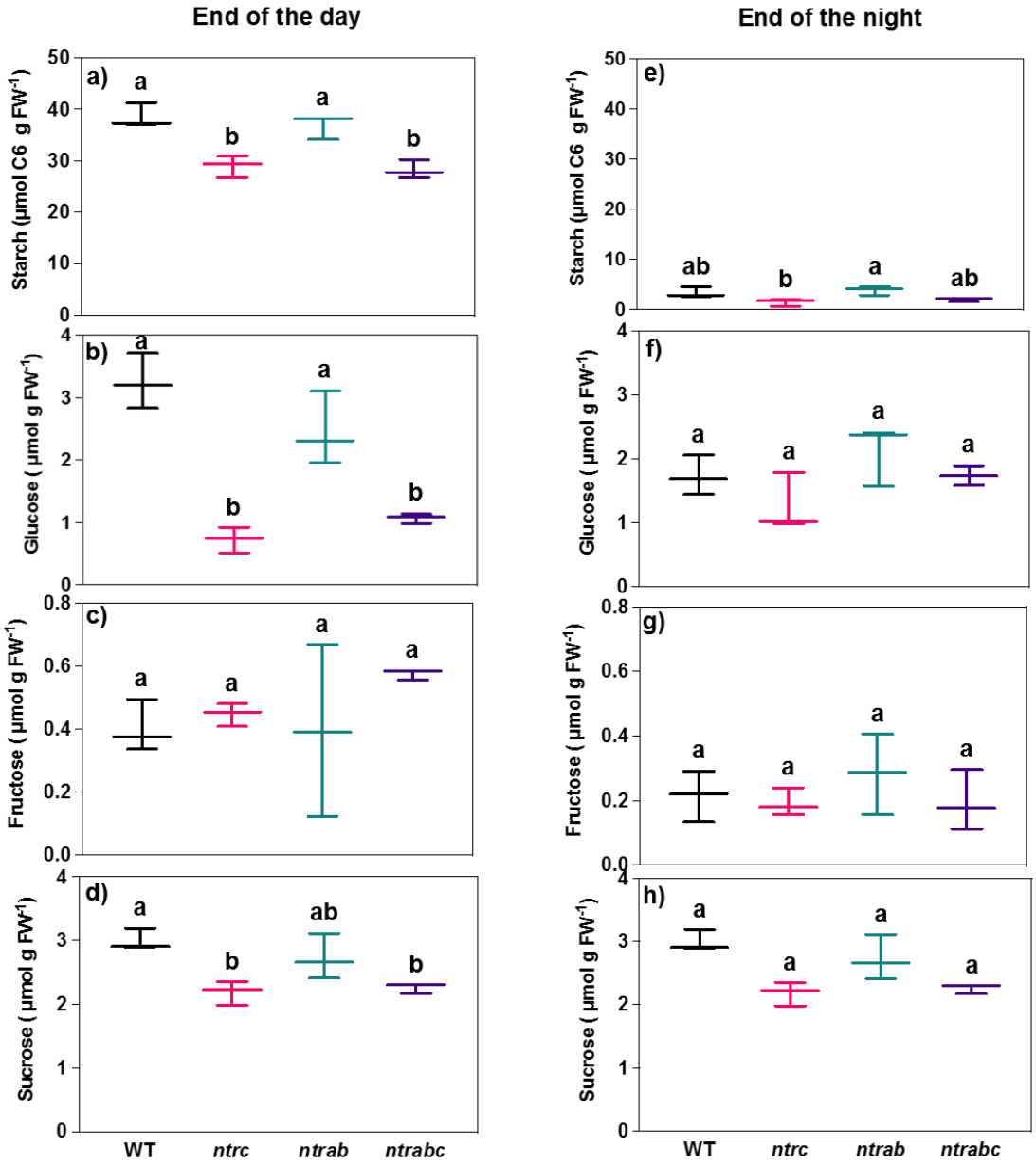

Figure S4 Concentration of carbohydrates in leaves of *Arabidopsis thaliana* L. wild type (WT) and mutants lacking NTRC (*ntrc*), NTRA and NTRB (*ntrab*) or all NTRs (*ntrabc*) harvested at end of the day (ED) (a-d) and end of the night (EN) (e-h) of plants grown under 125 µmol photons m^{-2} s^{-1}; 08:16 h photoperiod. Black, pink, green and purple box plots represent averages and standard errors of WT, *ntrc*, *ntrab*, and *ntrabc* genotypes, respectively (n = 3). Means that do not share a letter are significantly different according to ANOVA and Tukey test analysis ($P < 0.05$).

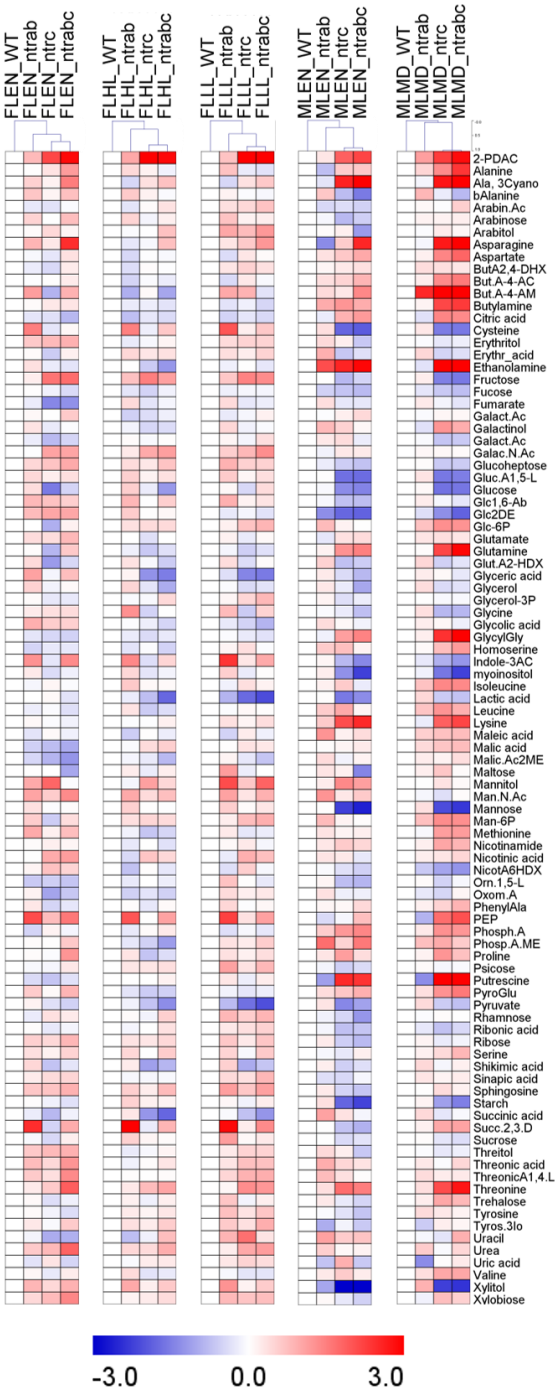

Figure S5 Heat map representation of the changes in the relative abundance of primary metabolites from *Arabidopsis thaliana* L. wild type (WT) and mutants lacking NTRC (*ntrc*), NTRA and NTRB (*ntrab*) or all NTRs (*ntrabc*). Plants were grown under moderate light (ML) (125 µmol photons m^{-2} s^{-1}, 12h/12h day/night photoperiod) and then transferred to fluctuating light (FL) conditions (1 minute of high light (HL): 500 µmol photons m^{-2} s^{-1} followed by 5 minutes of low light (LL): 50 µmol photons m^{-2} s^{-1}). After 4 weeks under ML, leaves were harvested at the mid of the day (MLMD) and at the end of the night (MLEN). Plants acclimated to FL were first grown for 3 weeks under ML conditions and then acclimated to 1 week of FL. After that, leaves were harvested at the low light (FLLL) and high light (FLHL) phases of the FL and at EN (FLEN). The average values of the relative abundance (normalized to ^{13}C-Sorbitol and fresh weight) were

normalized according to the WT values found at each condition and $\log_2$ transformed (n = 3-6). Heat map was carried out using MeV®.

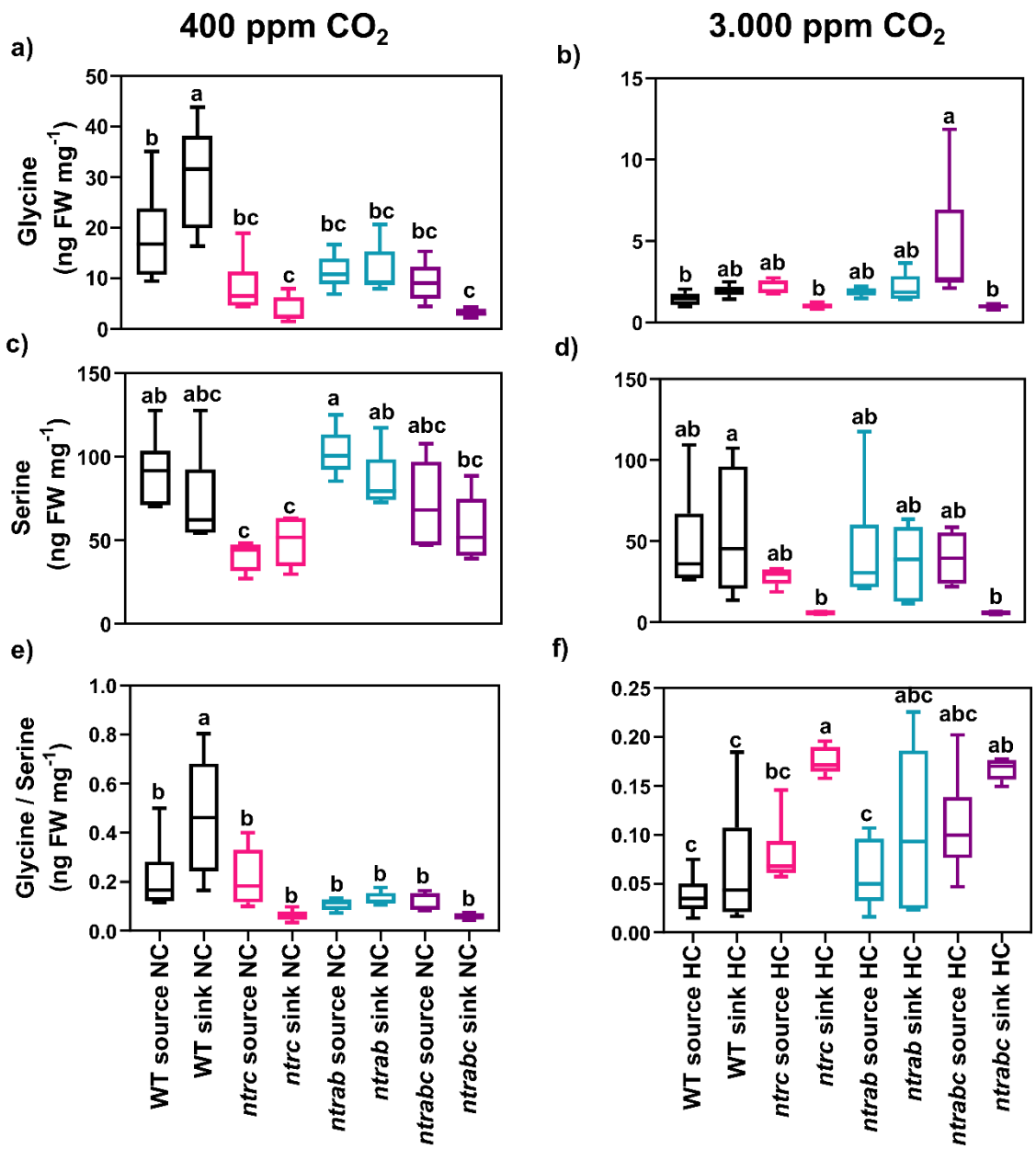

Figure S6 Concentration of glycine, serine and the ratio among them. Leaf metabolite concentration was obtained from 5-week-old *Arabidopsis thaliana* L. wild type (WT) and mutants lacking NTRC (*ntrc*), NTRA and NTRB (*ntrab*) or all NTRs (*ntrabc*) grown under 120 µmol photons m^{-2} s^{-1}, 12/12 h photoperiod and either ambient (NC, 400 ppm) or high (HC, 3000 ppm) CO_2 concentration. Box plots represent averages and standard errors of the concentration of the metabolites (ng mg^{-1} FW) identified by liquid chromatography mass spectrometry (LC-MS) in leaf samples harvested at the end of the day. Means that do not share a letter in each graph are significantly different according to ANOVA and Tukey test analysis ($P < 0.05$). The graphs were created using GraphPad Prism 9.

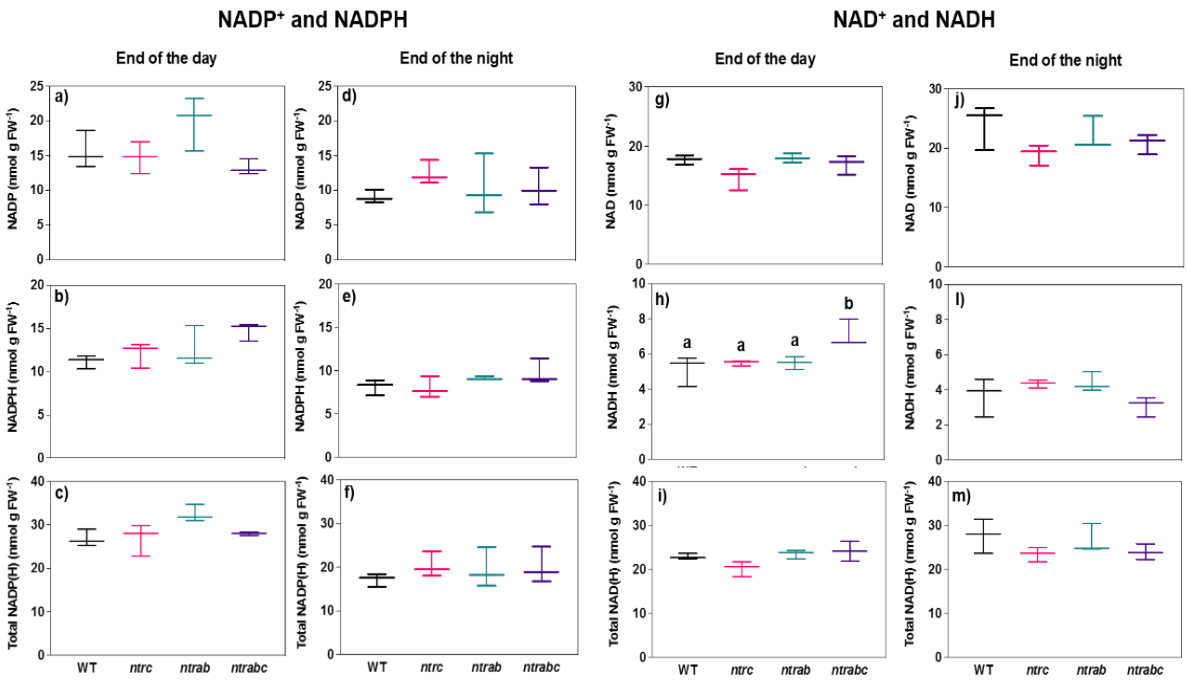

Figure S7 Concentration of pyridine dinucleotides in leaves of *Arabidopsis thaliana* L. wild type (WT) and mutants lacking NTRC (*ntrc*), NTRA and NTRB (*ntrab*) or all NTRs (*ntrabc*) harvested at end of the day (ED) (a-d) and end of the night (EN) (e-h) of plants grown under 125 µmol photons m^{-2} s^{-1}; 08:16 h photoperiod. Black, pink, green and purple box plots represent averages and standard errors of WT, *ntrc*, *ntrab*, and *ntrabc* genotypes, respectively (n = 3). No statistical differences were found between the genoytpes, with exception of the content of NADH at ED. Means that do not share a letter in figure h are significantly different according to ANOVA and Tukey test analysis ($P < 0.05$).

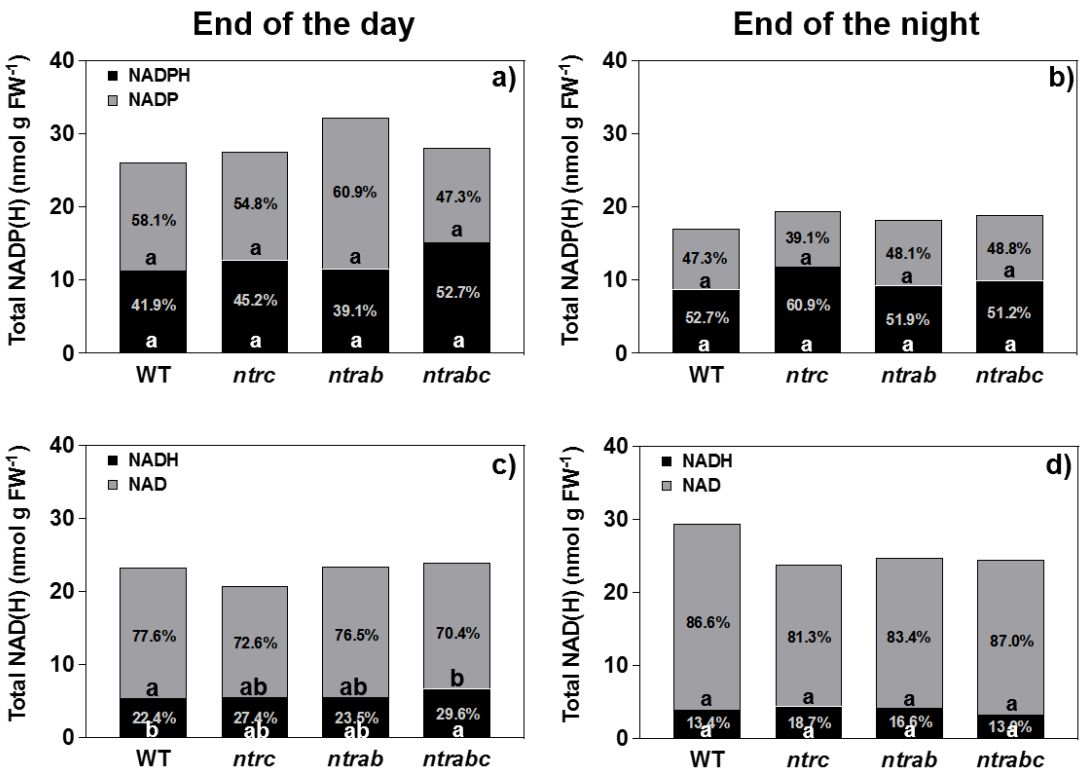

Figure S8 Redox status of pyridine dinucleotides in leaves of *Arabidopsis thaliana* L. wild type (WT) and mutants lacking NTRC (*ntrc*), NTRA and NTRB (*ntrab*) or all NTRs (*ntrabc*) harvested at end of the day (ED) and end of the night (EN) of short-day (125 µmol photons m^{-2} s^{-1}; 08:16 h photoperiod) grown plants. a-b) Percentage of NADP and NADPH related to the total NADP(H) concentration at ED (a) and EN (b). c-d) Percentage of NAD and NADH related to the total NAD(H) concentration at ED (c) and EN (d). Genotypes that do not share a letter within each parameter are significantly different according to ANOVA and Tukey test analysis ($P < 0.05$).

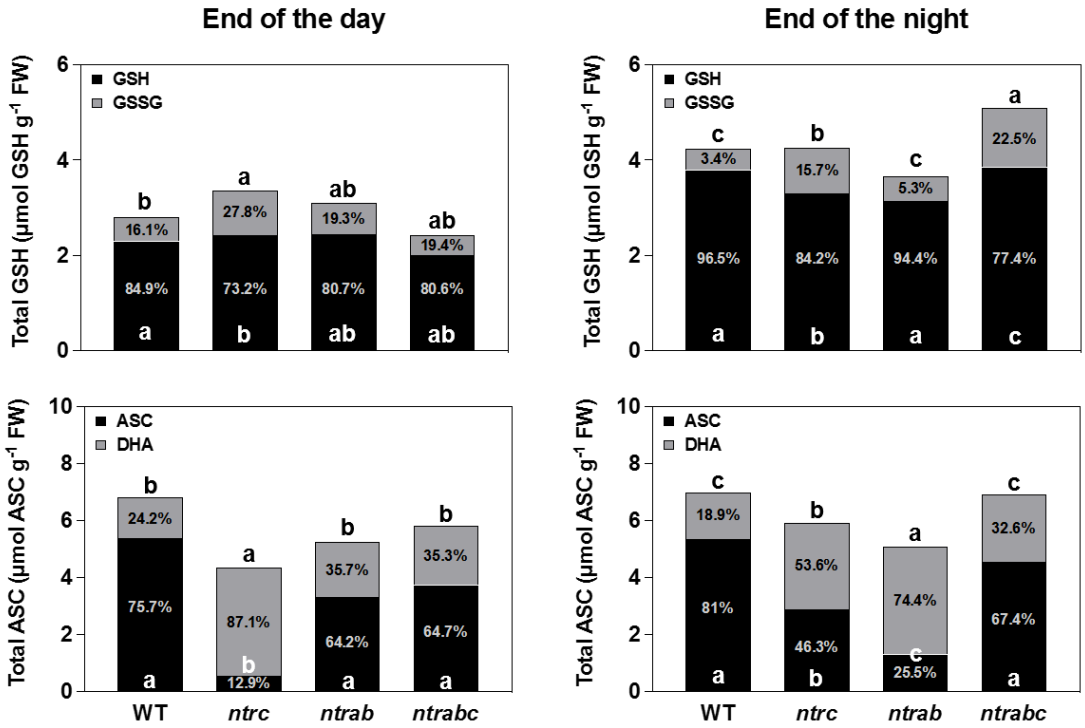

Figure S9 Redox status of glutathione and ascorbate in leaves of *Arabidopsis thaliana* L. wild type (WT) and mutants lacking NTRC (*ntrc*), NTRA and NTRB (*ntrab*) or all NTRs (*ntrabc*) harvested at end of the day (ED) (left figures) and end of the night (EN) (right figures) of short-day (125 µmol photons m^{-2} s^{-1}; 08:16 h photoperiod) grown plants. Genotypes that do not share a letter within each parameter are significantly different according to ANOVA and Tukey test analysis ($P < 0.05$). Abbreviation: ASC, ascorbate; DHA, dehydroascorbate; GSH, reduced glutathione; GSSG, oxidized glutathione.

Table S1 Photosynthetic characterization of *Arabidopsis thaliana* L. wild type (WT) and mutants lacking NTRC (*ntrc*), NTRA and NTRB (*ntrab*) or all NTRs (*ntrabc*). Gas exchange analysis were performed in fully expanded leaves of 8-week-old *Arabidopsis thaliana* L. wild type (WT) and mutants lacking NTRC (*ntrc*), NTRA and NTRB (*ntrab*) or all NTRs (*ntrabc*) using a portable infra-red gas exchange analyser. Abbreviation: Γ, CO_2 compensation point; *A*, net CO_2 assimilation rate; g_s, stomatal conductance; C_i, substomatal CO_2 concentration; *E*, transpiration rate; C_i/C_a, ratio between substomatal and ambient CO_2 concentration. Means that do not share a letter in the column are significantly different according to ANOVA and Tukey test analysis ($P < 0.05$) (n= 6 ± SE).

	Γ	***A***	g_s	C_i	***E***	C_i/C_a
	µmol mol^{-1}	µmol m^{-2} s^{-1}	mol m^{-2} s^{-1}	µmol mol^{-1}	mol m^{-2} s^{-1}	µmol µmol^{-1}
WT	66.13±10.52^{a}	8.32±2.0^{a}	0.21±0.05^{a}	319.31±14.0^{a}	4.13±0.3^{a}	0.85±0.06^{a}
ntrc	126.48±17.6^{b}	3.76±0.6^{b}	0.09±0.01^{b}	322.84±4.3^{a}	1.84±0.2^{b}	0.80±0.02^{ab}
ntrab	70.57±18.8^{a}	6.58±0.8^{c}	0.17±0.03^{c}	320.61±13.9^{a}	3.19±0.5^{c}	0.81±0.03^{ab}
ntrabc	122.96±33.2^{b}	3.25±0.8^{b}	0.07±0.02^{b}	315.98±13.8^{a}	1.50±0.3^{b}	0.79±0.4^{b}

Table S2 Description of the abbreviations of the metabolites displayed in the figure 7.

Abbreviation	Metabolite
Gln	Glutamine
Gly	Glycine
Orn	Ornithine
3PGA	3-Phosphoglycerate
CMP	Cytidine monophosphate
Asp	Aspartate
Glu	Glutamate
Met	Methionine
2-OG	2-Oxoglutarate
Ser	Serine
AMP	Adenosine monophosphate
Ala	Alanine
His	Histidine
Asn	Asparagine
Arg	Arginine
Pro	Proline
Val	Valine
Phe	Phenylalanine
Trp	Tryptophan
Lys	Lysine
GABA	γ-Aminobutyric acid
Tyr	Tyrosine
Leu	Leucine
Ile	Isoleucine
Thr	Threonine
Arg-Succ	Arginine-Succinic acid